Mechanical properties of cob-earth composites: variability and focus on the different calculation methods of Young's modulus

Philippe Poullain, Mircea Barnaure, Stéphanie Bonnet

Mechanical properties of cob-earth composites: variability and focus on the different calculation methods of Young's modulus

Philippe Poullain[a,*], Mircea Barnaure[b], Stephanie Bonnet[a]

[a] Nantes Université, Centrale Nantes, CNRS, GeM, UMR 6183, F-44600 Saint-Nazaire Cedex 1, France.
philippe.poullain@univ-nantes.fr, stephanie.bonnet@univ-nantes.fr
[b]Faculty of Civil Engineering, Technical University of Civil Engineering of Bucharest, Romania, Blv. Lacul Tei 122 - 124, 020396, Bucharest, Romania, mircea.barnaure@utcb.ro

*Corresponding author email: philippe.poullain@univ-nantes.fr

Highlights

- Cob mechanical properties are determined using monotonic and cyclic testing.
- Young's modulus is calculated through different methods: E_{cycle}, E_{tan}, E_{mono} and E_{dyn}.
- PDFs are obtained for compressive and tensile strengths, and Young's modulus.
- Standard deviation, COV, Q_1, Q_2 and Q_3 *quartiles*, IQR, outliers, $f_{5\%}$ are established.
- E_{cycle} is the most significant and increases with applied stress.
- Value of E_{dyn} is higher than E_{cycle}.

Abstract

Mechanical property data for earthen materials are currently lacking. Usually, only average values are available. This study investigates the mechanical properties (tensile and compressive strength, Young's modulus) of cob. The results obtained for different cob mixes with and without fibres are analysed. Four different moduli – E_{cycle}, E_{tan}, E_{mono} and E_{dyn} – are examined. Probability density functions, mean, standard deviation and percentiles are determined for each mechanical property. Value dispersion for all the properties studied is large and the difference between mean value and 5th percentile is 82%, 81% and 77% for tensile strength, compressive strength and Young's modulus, respectively.

Modulus values are highly dependent on the calculation method used. E_{cycle} obtained during the unloading phase of the cyclic compression test is more relevant than E_{tan} and E_{mono} because only elastic deformations occur. The modulus increases with applied stress (from 120 to 327 MPa for specimens without fibres and from 70 to 232 MPa for specimens with fibres) highlighting the evolution of material microstructure during loading. E_{dyn} is higher than E_{cycle}: the average dynamic Young's modulus is 6917MPa without fibres and 2088MPa with fibres.

Keywords: earthen composites, fibre, compressive and tensile strength, Young's Modulus

Declarations of interest: None

1. Introduction

Earth has been used as building material for a very long time [1]. Over the last century, this raw material has been gradually replaced with modern standardised materials in developed countries. However, in the last 20 years, there has been a resurgence of interest for the use of earth in construction, which may be explained by the perception of earth as a building material with very low environmental impact [2].

The use of uncompressed non-stabilised earth with or without the addition of fibres is generally associated with the idea of locally available materials [3]. Earth composition and earth composite formulation can vary significantly depending on the site. As shown by Verron *et al.* [3], Rojat *et al.* [4] or Hamard *et al.* [5], various test parameters are found in the literature:

- *Soil composition:* some studies [6-9] address the usability of different soils for different construction techniques, whereas others [10-12] conclude that soil composition alone (silt, clay and sand content) is not relevant for assessing material usability and strength.
- *Water content:* as demonstrated by Champiré *et al.* [11], this parameter affects mechanical strength. Three soil types have been analysed for water contents between 25%-95%. The results show that compressive strength decreases with higher water contents for all the soils considered (sandy, loamy and clayey soils).
- *Fibres* are traditionally used in adobes and cob [13] because they reduce shrinkage [14] and improve material mechanical behaviour. An increase in strength is observed with the increase in fibre percentage [15-18]. However, strength starts decreasing above a certain content value. This threshold depends on fibre type.

For all these reasons, raw earth properties are highly variable [19-21].

Despite this widely recognised variability, many recent studies investigating earth mechanical properties are still based on a limited number of specimens. Moreover, results cannot be directly compared because specimen size and testing methods are different. Consequently, results differ significantly as underlined by Champiré *et al.* [11], Illampas *et al.* [22] and Rodriguez-Mariscal *et al.* [23]. While most studies are based on specimens made in the laboratory, some are based on samples taken from existing buildings. The study conducted by Azil *et al.* [24] shows that significant differences are observed between properties measured on-site and results obtained in the laboratory.

Among the different studies considered, some findings are discussed in the next paragraph. The discussion focuses particularly on:

- compressive strength (Table A1);
- tensile strength (Table A2);
- Young's modulus (Table A3).

The tables in the appendix present the published results discussed in this paper, with a special emphasis on number and size of specimens and coefficient of variation.

Regarding ***compressive strength***, the published results found in [3,11,14-16,18,22-23,25-29] are analysed and summarised in Table A1. Although all values given relate to compressive strength, results are not directly comparable since tests have been carried out on cylindrical, cubic or prismatic specimens of different sizes. Most studies propose an average value based on test results for only 3 or 4 specimens. The coefficient of variation (CV) is not always calculated and, when it is, few values are given and sometimes only as figures. Reported CV may vary widely between studies and even within one given study. Miccoli *et al.* [25], for instance, report a CV of 2% for tests performed on cob, a material characterized by its variability. At the upper end of the range, the tests performed on samples extracted from existing buildings [26] give CV values as high as 95%. In [22], tests have been carried out on adobes from a local traditional producer and the CV values obtained range from 3 to 77%. The authors explain that the variability in test results may be accounted for by large differences in material composition between batches.

Regarding ***tensile strength***, few studies are available and most studies carried out on earth-based materials are dedicated to the examination of compressive strength as in the study by Cardenas-Haro *et al.* [19]. A number of studies [3,14,18,27,29-31], in which tensile strength has been calculated using bending testing, are examined and results summarised in Table A2. It is observed that a general small number of tests has been conducted. CV values are very often not reported or given in the form of figures. Yet, these values range from 13% to 36% for laboratory specimens [3,30] and from 24% to 51% for samples taken from existing buildings [27].

We also note that, when compression tests are carried out, ***Young's modulus*** is often calculated. The results presented in [3,11,15,22-23,25-29,32] are examined and summarised in Table A3. No consistent methodology for the determination of Young's modulus and the interpretation of results has been found.

In [25], the specimens tested vary in size, while Young's modulus is calculated according to DIN 1048-5 [33], a German standard that is normally used for concrete elements. Depending on specimen size and mix

composition, values are between 650-2200 Mpa. Regarding CV, the calculated value is only 3% for earth blocks, but reaches 68% for cob specimens.

In [15], tests are carried out on specimens of two different sizes for various earth compositions. Values are then between 98-211 MPa and 58-94 MPa, respectively for the smallest and the largest specimens. CV, calculated from eight specimens for each mix, ranges between 17% and 45%. The highest value is obtained for earth specimens with no fibres. They also have the highest modulus value. Although values are provided here, the way Young's modulus has been calculated from the stress-strain curves is not specified.

In [23], the tests to determine Young's modulus have been carried out on cubes, prisms and cylinders. Regarding cubes, displacements are measured using a loading device, while prisms and cylinders have been equipped with probes. Consequently, two different stress-strain curves are plotted and three different modulus values are obtained from each stress-strain curve: $E_{1/3}$, $E_{2/3}$ and E_m:

- $E_{1/3}$ and $E_{2/3}$ represent the secant modulus obtained at 1/3 and 2/3 of compressive strength, respectively;
- E_m is the slope of the chord between 1/3 and 2/3 of maximum compressive strength.

Young's modulus values displayed by the loading device are within the range 21-60 MPa for cubes, 77-132 Mpa for prisms and 78-195 MPa for cylinders. When displayed by sensors, modulus values are much higher between 557-1081 MPa for prisms and 802-1539 MPa for cylinders. Regarding variability, calculated CV ranges from 11% to 72%. This study is of relevance in terms of number of prismatic specimens tested (22 specimens, a much larger number than most studies). Nevertheless, CV values still range between 32%-60% (depending on Young's calculation methods).

In [26], an average of five samples from existing buildings has been tested for each building. The modulus calculation method is not specified. The values proposed are between 51-448 MPa. CV values do not appear, but the standard deviation appears in the figures. From these figures, we calculate the corresponding CV values. They range between 7%-139%, most being greater than 70%.

Samples from existing houses have also been tested by Silveira *et al.* [27]. Two values of Young's modulus based on stress-strain curves obtained with cylindrical specimens during monotonic loading: secant modulus, $E_{1/3,}$ at 1/3 of peak stress and secant modulus, $E_{peak,}$ at peak stress.

Calculated values are between 1500-2500 MPa for E_{peak} and 9000-17500 MPa for $E_{1/3}$. These values are high (compared with published data) because deformations are measured directly on specimens, not with the measuring device. Given the shape of the stress-strain curves, Young's modulus calculation as the secant modulus at peak stress appears inconsistent. Regarding variability, CV values are between 28%-45%, a range, however, obtained with very few data.

In [22], Young's modulus has been calculated from strain-stress curves as the secant modulus between 5% and 50% of the maximum stress during monotonic loading. This choice assumes that most specimens have a linear behaviour in this displacement range. This study focuses on the results obtained with cylindrical, prismatic and cubic adobe specimens using different testing methods (load-control and displacement-control). The average values for the two types of adobes considered are 32 and 37 MPa, respectively. CV values are 72% and 45%, respectively. According to the authors, the high CV values may be due to significant differences between soil batches.

In [28], Young's modulus is measured on the linear part of the strain-stress curves. However, the corresponding stress or strain range is not specified. Values are between 31-134 MPa for the specimens with fibres. A 502 MPa average value is proposed for raw earth specimens. Regarding variability, CV values for specimens with fibres are low (3% to 8%). CV is 34% for raw earth specimens, a value, however, obtained from three specimens only.

In [11], a loading protocol including successive loading-unloading cycles with 20%, 40%, 60%, and 80% increasing stress levels up to the expected maximum stress level was applied (one loop for each cycle). In order to estimate this expected maximum value, some preliminary tests have been conducted with monotonic loading. Cycle choice is based on the consideration that only elastic strain occurs during the unloading phase. Young's modulus decreases with successive loading cycles from 2460 to 2000 MPa depending on the earth material. These results, however, have been obtained with only three samples from existing rammed earth century-old buildings.

In [32], the mean value obtained from double flat jack tests performed on cob specimens is 176 MPa for slope modulus and 203 MPa for secant modulus. CV values are 49% and 43%, respectively.

2. Objectives and approach

The literature reviewed for this paper reveals that there is no consensus on test methods or specimen size for the assessment of earth composite mechanical properties, Young's modulus in particular. In addition, focusing only on average values, the current approach could be misleading as to the actual properties of materials possibly used in building construction. This is particularly true because standardised modern material design is based on the characterisation and not on the average values of properties.

This paper presents the results obtained for raw earth composites prepared according formulations traditionally used for cob (earth mixed with natural fibres), but produced like adobes in the laboratory. Compressive and tensile strengths, and Young's modulus are determined by compression and bending testing. Comparisons are made between Young's modulus and dynamic modulus obtained by non-destructive testing. In addition, different

approaches used to determine Young's modulus using monotonic or cyclic compression testing methods are also discussed. Finally, a statistical analysis of the results is conducted and the distribution functions for these parameters are determined.

For the purpose of the present analysis, the focus is not on average values obtained for material properties. As mentioned above, different soil compositions, different fibre types and contents, different moisture levels and different construction techniques will result in some mean values that may vary substantially. The objective of this research is to examine the general approach in terms of sampling, test methods and data treatment, with a particular emphasis on result variability.

3. Materials and Methods

3.1. Materials

3.1.1. Earth

The soil used for the study is a waste material collected at the "Maison Neuve" eco-district in Guérande, France. Soil particle size distribution (Figure 2-a) is determined according to NF EN ISO 17892 [34] using:

- wet sieving for particle diameter greater than 80µm
- sedimentation for the other particles.

The soil is a sandy loam composed of 8% clay, 47% silt and 45% sand. Because earthen material assessment is commonly based on the textural triangle diagram [4,5], Figure 2-b presents soil classification according to the French soil science organisation "GEPPA" [35]. On the GEPPA diagram, silt fraction upper diameter limit is 50µm, which is lower than the 60µm limit considered in [34]. Thus, silt content is 44% and sand content is 48%. On the texture triangle:

- grey areas are mentioned in [4] as generally considered suitable for rammed earth;
- green dots are values obtained for samples taken from existing rammed earth houses [4];
- green areas correspond to textures observed by [5] on cob buildings in Brittany (France);
- red dot corresponds to the soil studied.

Atterberg limits are determined according to NF EN ISO 17892-12 [36]. Plastic limit is W_P=17% and liquid limit is W_L=34%. Plasticity index is I_P=17. Methylene blue value is 1.9 and determined according to NF EN 933-3+A1 [37].

a)

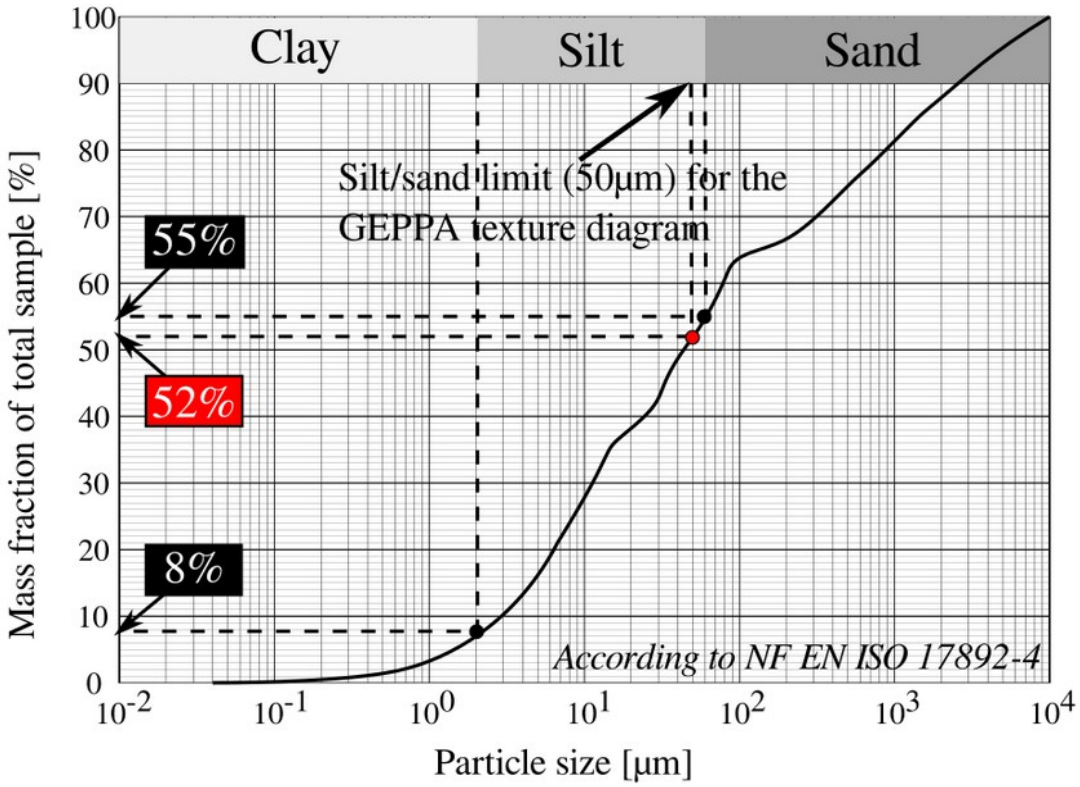

b)

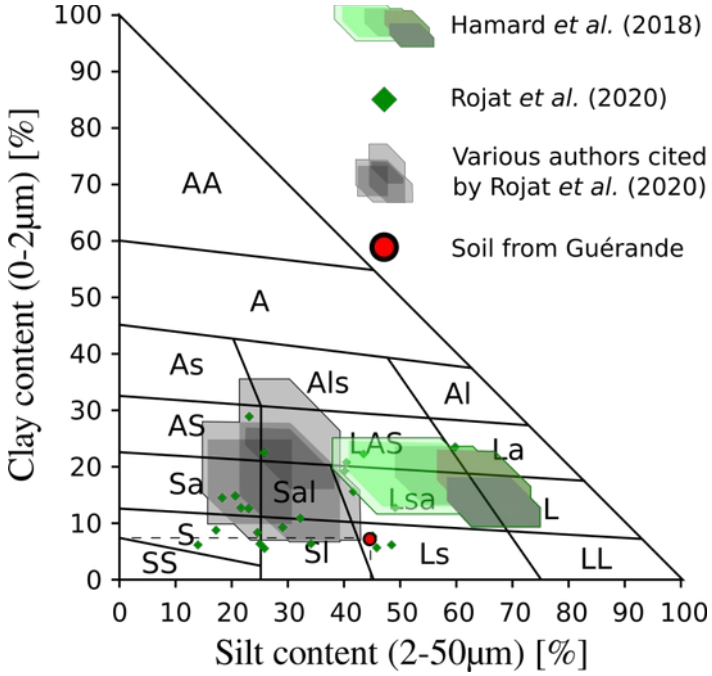

Figure 1: Particle size distribution of studied soil (a) and textural triangle diagram (b) –red dot corresponds to the soil taken in Guérande (sandy loam)

3.1.2. Fibres

In this paper, the word "*fibres*" refers to any part of the plant stems (whole stem, fibre or woody parts). The fibres used are hemp shives (commercial product Chanvribat – Figure 2-a) and reeds produced locally (Figure 2-b). Both types of fibres appear in the literature as traditionally used for earthen constructions [13]. The length and width of hemp shive particles have been determined using 2D image analysis in a previous study [38]: hemp particles average 8.9 mm in length and 2.0 mm in width. Reed, with an average diameter of 3.5 mm, is cut into approximately 200mm sections then mixed using a kneading hook (Figure 2.a). This 200-mm length is commonly

used for craft cob constructions. However, during mixing, the reed fibre length decreases. Length reduction is assessed by measuring the length after different mixing times (number of revolutions of the kneading hook – Figure 3.b). The final reed average length is 20mm. In this study, formulations including natural fibres are chosen with 8% fibre content by mass (Figure 2-c). This percentage is traditionally used in the Loire-Atlantique area (France) for cob buildings and has been chosen after discussion with experts involved in earth building construction with practical skills. The high fibre content makes it possible to differentiate between raw earth and fibre mixes for all properties measured.

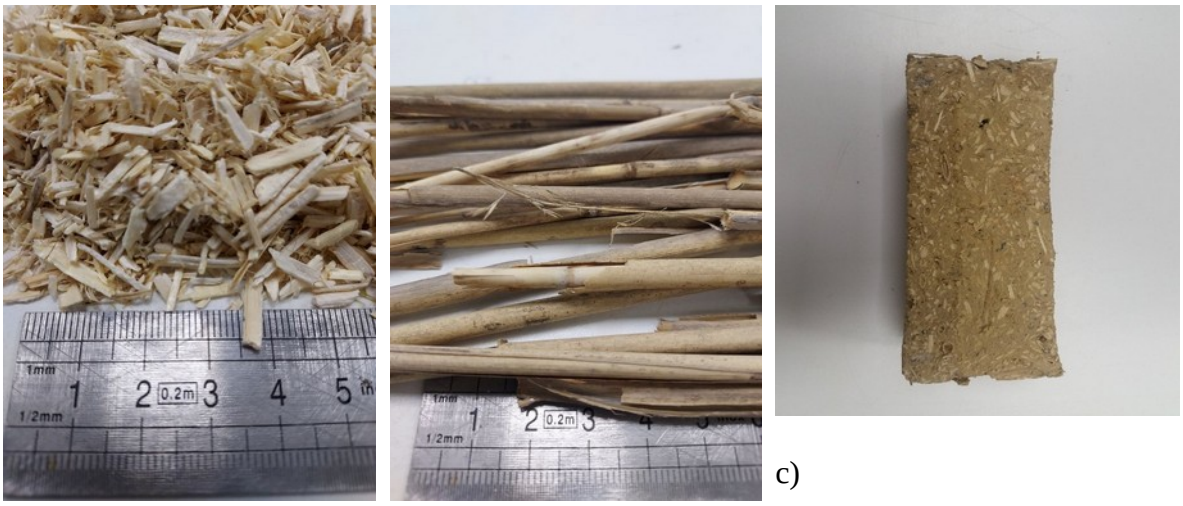

a) b) c)

Figure 2: Different materials used in the study a) hemp shives – b) reed – c) picture of a specimen with fibres where earthen matrix, reed and hemp shives can be clearly seen

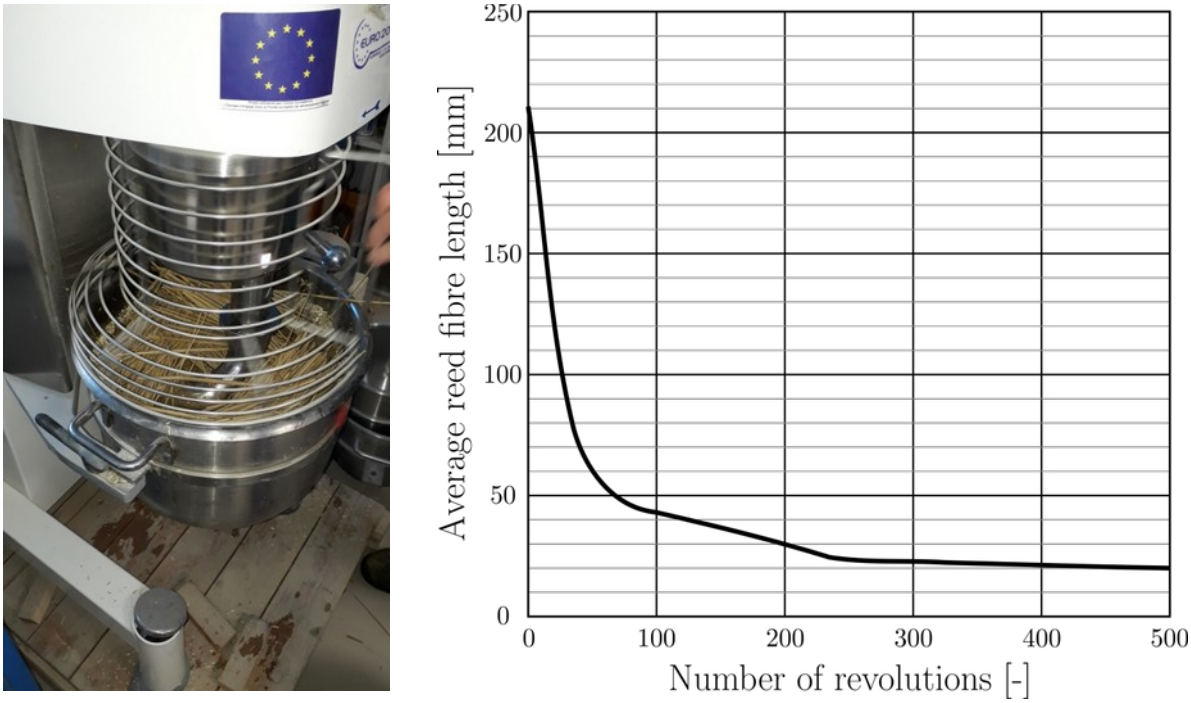

a) b)

Figure 3: Kneading hook (a) – reed length evolution *vs* number of revolutions of the kneading hook (b)

3.1.3. Specimen preparation and curing

The amount of material in the mix is established according to the knowledge of local experts. A 2:2:1 volume ratio of raw earth, hemp shives and reed is used. Fibres represent 8% by mass on the total mass of the mix (7% hemp and 1% reed). Raw materials are placed into a large steel bowl and are mechanically mixed using a kneading hook at low speed (30 rpm) while gradually adding water to the mix until desired consistency is reached (Figure 2.a). Initial water content is checked after drying the specimens in the oven (50°C) until the mass has stabilised. Water content obtained is 23% for raw earth material and 24% for the raw earth and fibres mix.

The specimens are cast into 31×19×5.3cm parallelepipedal wooden moulds placed on a wooden tray (Figure 4). Earth is thrown into the mould one handful at a time. For each mix, with and without fibres, three slabs are made. After demoulding, the earthen slabs are cut into six pieces with average dimensions of 5.17×5.3×19cm (Figure 2). Eighteen specimens without fibres and eighteen with fibres are obtained.

After casting, the specimens are dried naturally to constant mass in a climate chamber where temperature (20°C) and relative humidity (50%) are kept constant. In spite of the initially high water content, no cracks formed during the period of slow drying.

a)

b)

Figure 4: Preparation (a) and cutting of the fresh slabs to obtain six specimens (b)

Because water content significantly affects earthen material properties [11], [39], tests are carried out at 20°C and with 50% relative humidity. At the time of testing, the water content is 3.1% for earth specimens and 3.3% for earth-fibres specimens, corresponding to the equilibrium water content at 20°C and 50% RH.

3.2. Mechanical characterisation

3.2.1. Bending and compression tests

In order to address soil behaviour during bending and determine tensile strength, the specimens are subjected to 3-point bending tests using a Zwick Z50 press (50kN maximum load – Figure 5). Tests are conducted at prescribed speed of 10mm/min. Stress σ_b is obtained from Equation (1), where F is the force (N), L the distance between supports (100 mm), a the specimen width (m) and b the specimen height (m), as:

$$\sigma_b = \frac{3FL}{2ab^2} \quad (1)$$

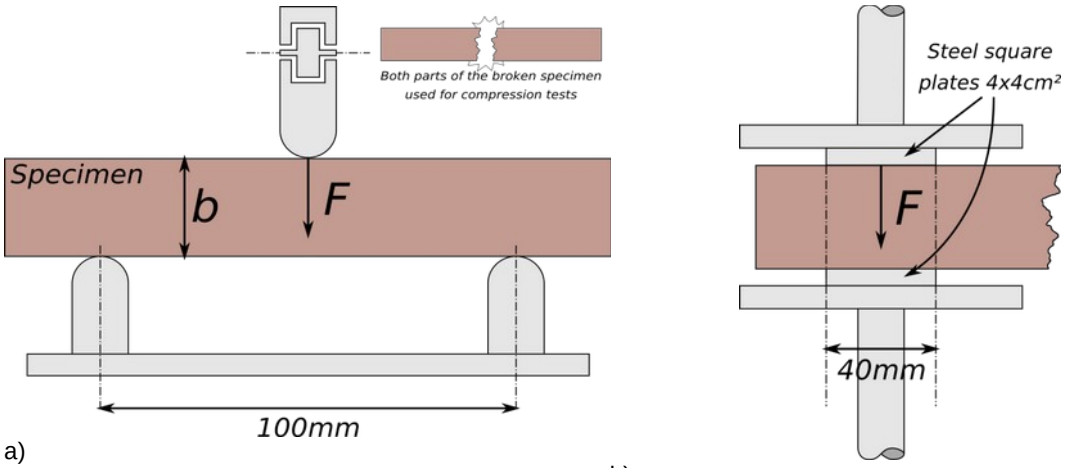

a) b)

Figure 5: Experimental setup for three-points bending testing (a) for monotonic or cyclic compression testing (b)

Compression tests are carried out using the same Z50 Zwick press. During the bending test, the specimen has broken in two. Both pieces are then tested for compression strength. Two 40x40mm steel square plates are placed between the two parallel sides of the specimen and the press plates (Figure 5b). The applied stress σ_c is obtained from Equation (2), where F is the applied load (N) and d the square plate length (d = 0.040 m), as:

$$\sigma_c = \frac{F}{d^2} \quad (2)$$

For both bending and compression tests, longitudinal displacements are recorded during the loading phase. Flexural strain is calculated according to the following formula:

$$\varepsilon_f = \frac{6bs}{L^2} \quad (3)$$

where s is the measured displacement (m).

Tensile strength R_f and Compressive strength R_c are defined as maximum tensile and compressive stress values, respectively.

The first 16 (2x8) specimens of each mix (with and without fibres) are tested in compression through a monotonic displacement increment until failure. Cyclic load testing is carried out on the remaining 20 (2x10) specimens of each formulation. These tests apply a series of five stress loops (loading and unloading) for five different stress values (Figure 7-a). Each loading phase is followed by a full unloading phase down to 0 kN. After the last loading loop at the maximum stress value is applied, compressive stress is increased until the specimen fails. As compressive strength is obviously not known *a priori* for each specimen, the stress values for cyclic testing are

set at respectively 3.75%, 7.5%, 15%, 30%, 60% of the mean compressive strength obtained during monotonic testing performed on the previous 16 specimens of the same formulation. The value of the compressive strength is assumed to be independent of loading mode (monotonic or cyclic) and will be discussed in Section 4.

3.2.2. Young's modulus determination

As explained in [40] and [41], different methods can be used to determine Young's modulus for hemp concrete. In these papers, the authors mention different values Young's modulus calculated on different parts of the stress/strain curve or examine different approaches, like initial modulus E_{ini}, secant modulus E_{sec}, tangent modulus E_{tan} or cycle modulus E_{cycle}. These works show that hemp concrete presents a non-linear behaviour with varying Young's modulus values during compression. They also highlight the fact that, given this complex behaviour and the lack of common methodology for the determination of Young's modulus regarding hemp concrete materials, studying how methodology affects this mechanical parameter is necessary. In fact, for materials with complex mechanical behaviour, the slope value of the stress/strain curves measured during compression tests cannot be considered as the material Young's modulus value. Several effects, indeed, may combine during compression, like elastic and plastic deformations, damaging or density evolution. Consequently, the only time Young's modulus can be determined is during the unloading phase when only elastic deformations occur. This justifies the choice of cyclic compression testing.

Similar observations can be made about earthen composite non-linear behaviour [42]. In the present study, Young's modulus E is determined using different methods. During the monotonic tests on the first specimens (Figure 6), a non-linear relationship between applied stress and strain has been established. In order to analyse loading protocol impact on behaviour under compressive loading, both monotonic and cyclic protocols are used. Young's modulus is thus obtained from the stress-strain curves using different methods:

- *From monotonic compression testing (E_{mono}):* Young's modulus E_{mono} is the slope of the stress-strain curve on the most linear part of the curve (Figure 6) estimated by least squares approximation. Sixteen Young's modulus values are obtained for each formulation;
- *From cyclic compression testing (E_{tan}):* Young's modulus is calculated on the ramp before the cycle at the highest stress level is applied (E_{tan} in Figure 7-a) as the slope of the stress-strain curve called the ramp Young's modulus.
- *From cyclic compression testing (E_{cycle}):* Young's modulus E_{cycle} is obtained from the stress-strain curve during the unloading phase of each loop (five values for each stress level) as the slope of the curve calculated using 50% of the central values recorded during unloading using the least squares method (Figure 7-b). Young's modulus is determined only for the unloading phase because only elastic deformations occur, as mentioned above. For all the formulations (with and without fibres), 100 Young's modulus values (5 loops x 20 specimens) are obtained for the five different stress levels.

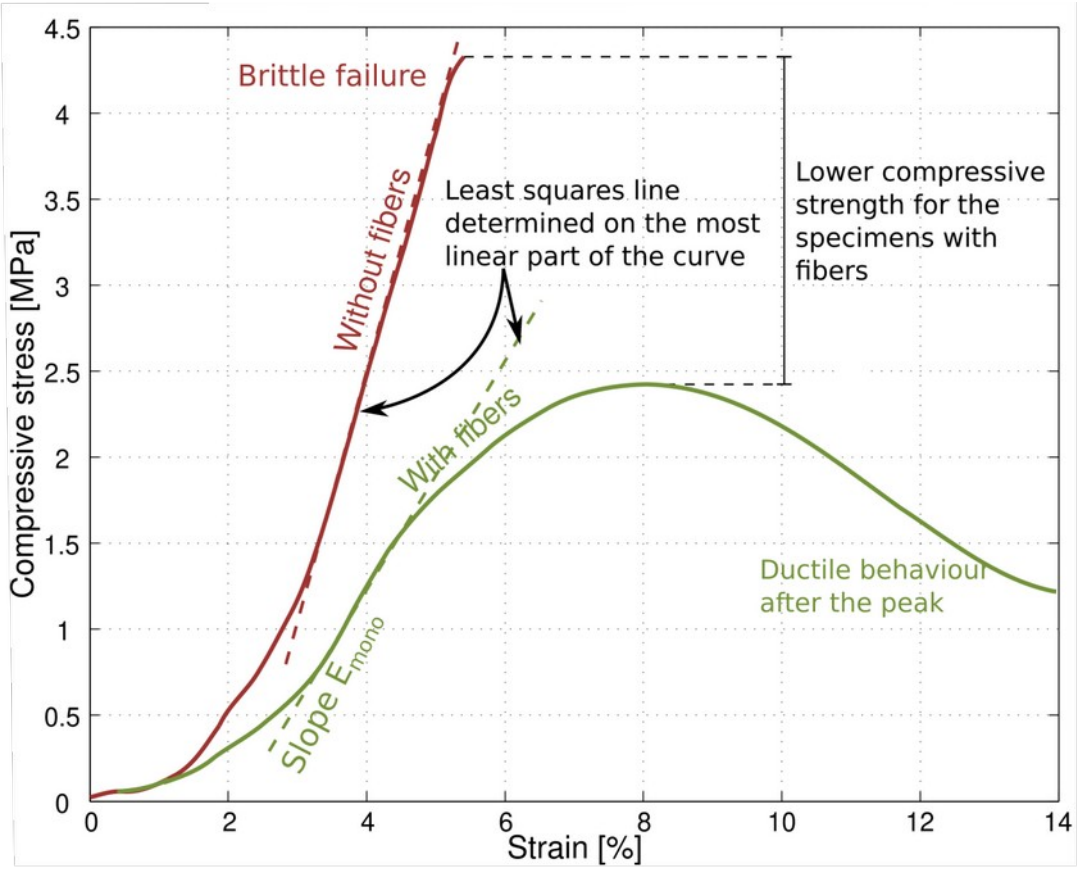

Figure 6: Example of stress-strain curves obtained during monotonic compression testing and method used for the determination of Young's modulus: specimens E2.1.4a (without fibres, in brown) and E1.2.1b (with fibres, in green)

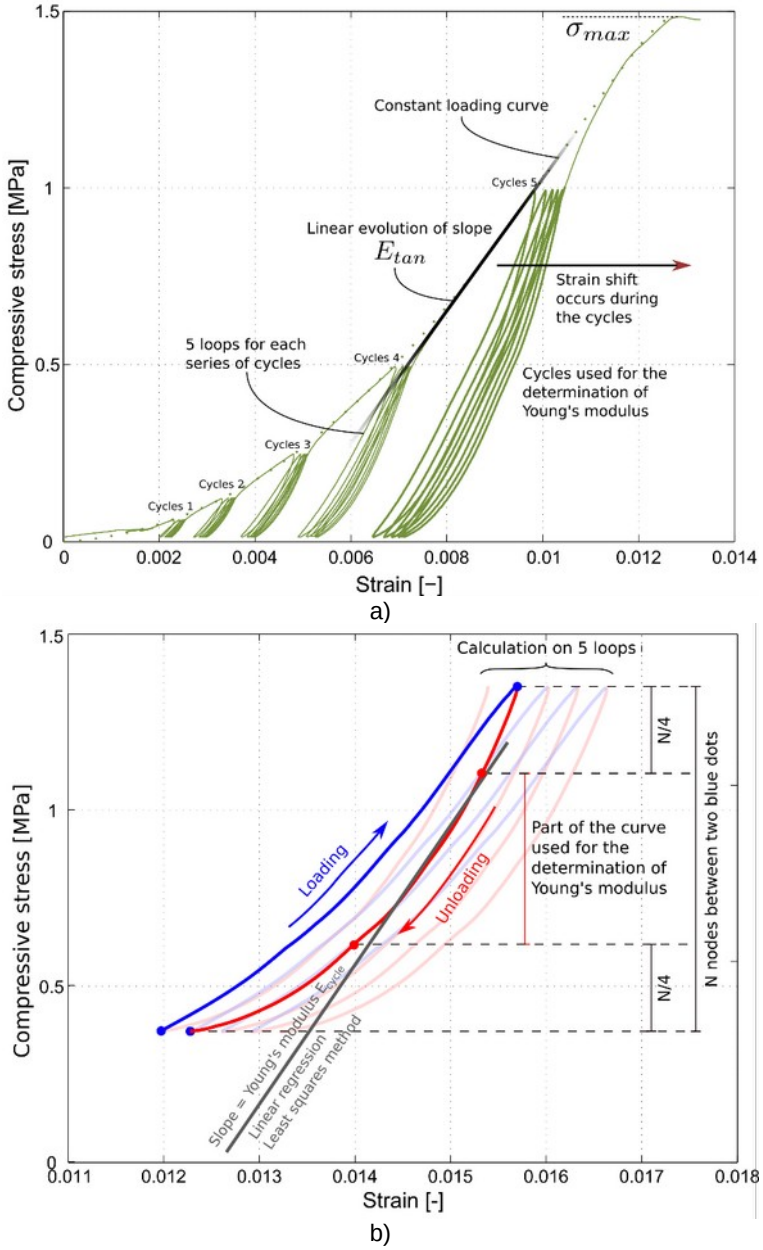

Figure 7: Cyclic compression testing and determination of Young's modulus for the fibred specimen E1.2.4a from the ramp slope before the highest stress level loops (a) –dotted line represents the assumed stress-strain curve corresponding to monotonic compression testing – and from the slope of the loop unloading phase inside a cycle (b)

3.2.3. Dynamic modulus

The dynamic modulus E_{dyn} is determined using Impulse Excitation Technique (Grindo Sonic). This non-destructive measurement method has already proved very simple and highly accurate [43]. The Grindo Sonic instrument records vibrations, performs time domain analysis and measures the natural frequency of the dominant vibration mode against a precision reference oscillator. The dynamic modulus is calculated from dimensions, mass and frequency measured for each specimen using Equation (4) in accordance with ASTM E1876-01 [44].

In Equation (4), E_{dyn} is Young's modulus (Pa), m is the bar mass (g), b the bar width (mm), L the bar length (mm), t the bar thickness (mm), f_f fundamental resonant frequency of the bar in flexion (Hz) and T_1 a correction factor that accounts for the bar finite thickness, Poisson's ratio, and so forth. We obtain:

$$E_{dyn} = 0.9465\left(\frac{m f_f^2}{b}\right)\left(\frac{L^3}{t^3}\right)T_1 \quad (4)$$

3.3. Statistical analysis

3.3.1. Mean and standard deviation

Mean m and standard deviation s of a measured parameter ε_y can be calculated directly from the N experimental data as follows:

$$m = \frac{1}{N}\sum_{i=1}^{N} \varepsilon_{yi} \tag{5}$$

$$s = \frac{1}{N}\sum_{i=1}^{N} (\varepsilon_{yi} - m)^2 \tag{6}$$

3.3.2. Statistical indicators

For the statistical data description, both average value μ and standard deviation σ are calculated from the experimental data. The coefficient of variation (CV), defined as the ratio of μ to σ , is also calculated. The three quartiles Q_1, Q_2 (median) and Q_3 are determined to display boxplots using Matplotlib. This Python plotting library also displays outlier values (Figure 8), *i.e.*, values outside the range $[Q_1\text{-}1.5\ IQR;\ Q_3\text{+}1.5\ IQR]$, where IQR=$Q_3$-$Q_1$ is the interquartile range.

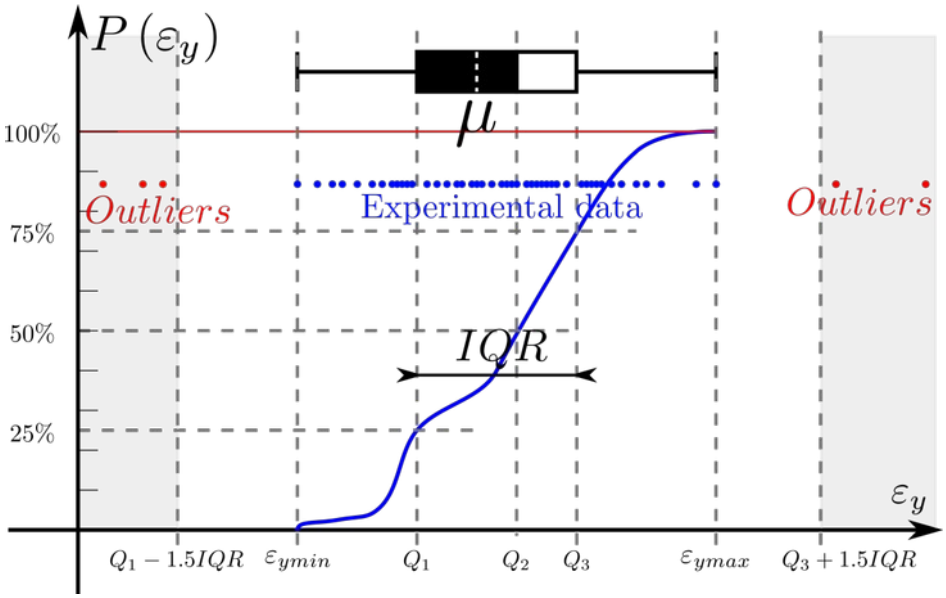

Figure 8: Boxplot statistical description of parameter ε_y –statistical indicators are determined by discarding values outside the interval $[Q_1\text{-}1.5\ IQR;\ Q_3\text{+}1.5\ IQR]$, where IQR is the interquartile range

3.3.3. Determination of the distribution functions

The parameter values obtained from the experiment (compressive strength, tensile strength, static Young's modulus, dynamic Young's modulus) are analysed to determine the probability density functions (PDFs). The range of the experimental data is determined and divided into an optimal number of intervals n_i defined by Sturges' law [45] and based on the total number of values N:

$$n_i = 1 + 3.322 \log(N) \tag{7}$$

This method is particularly suitable for data with a small number of values. Moreover, it assumes normality of data, a hypothesis that can be verified with the experimental data of one parameter. Then, PDFs are calculated using the Python module *scipy.stats.* The *scipy.optimize* module is used to calculate the parameters of the fitted normal law, *i.e.,* the mean μ and the standard deviation σ as:

$$f(x;\mu,\sigma) = \frac{1}{\sigma\sqrt{2\pi}} \exp\left[\frac{-(x-\mu)^2}{2\sigma^2}\right] \tag{8}$$

This solution is used to determine an estimate of the value $f_{5\%}$, which represents the value for which only 5% of the values will be lower, as:

$$f_{5\%} = \mu - 1.645\,\sigma \tag{9}$$

The choice of $f_{5\%}$ reflects the fact that this value is considered as a "characteristic" value for the structural design of building elements [46].

4. Results and discussion

4.1. Mechanical properties

4.1.1. Bending tests

The stress-strain curves obtained from bending testing are plotted in Figure 9. For clarity, the raw data for the 18 specimens tested are displayed in Figure 9-a. Figure 9-b shows a focus on two specimens to highlight the characteristic curve shape for two representative specimens and underline the differences in tensile behaviour between both formulations.

Tensile strength is greater for specimens without fibres than for those with fibres, which demonstrates that adding fibres has a negative impact on it. Regarding maximum tensile strength, it is 2 MPa for raw earth and 1.20 MPa for the fibre mix. The addition of fibres, therefore, induces a decrease by about 45% compared to the average value obtained for reference earth. This is not consistent with the results obtained in [16,17] for tests carried out on compressed earth blocks with low fibre content (0, 0.25%, 0.5%, 0.75% and 1%) for three different fibre types (coconut, palm oil and bagasse). The authors, indeed, conclude that fibre content and soil type do not affect tensile strength. In [31], tests have been conducted on hemp specimens with different fibre contents (2% and 3%) and fibre lengths (10, 20 and 30mm). Results show that tensile strength is higher with a 3% fibre content, and that, for this amount, specimens made with 30-mm long fibres have the highest tensile strength. Similarly, the analysis in [47] concludes that fibre content has a positive influence on the mechanical properties of compressed earth blocks made of raw earth and kenaf fibres of various lengths and fibre contents. It can be noticed, that in all three studies, fibres used are very thin (diameter lower than 1mm before mixing) and fibre contents are low. Consequently, the fibres are well distributed in the mixture, resulting in a homogeneous material with no defects or weak bonds between the fibres and the earthen matrix. Bouhicha *et al.* [14] also stress the positive influence of fibre addition with a tensile strength increase of 20 to 25% for specimens made of raw earth and 3.5% straw. However, the length of straw fibres is not uniform (from 10 to 500mm) whereas whether the longest fibres broke or not during mixing is not specified.

In the present study, fibres are thicker and may be considered as coarse plant aggregates more than thin fibres. Fibre content is high (8%), and the technique used is different (cob versus compressed earth blocks). This may account for the differences regarding the impact of fibre content on tensile strength. With coarse aggregates, bonds between earthen matrix and fibres:

- are weaker due to the aggregate higher porosity at the fibre/matrix interface (voids);
- are less: contact surface between fibres and matrix is smaller.

However, the addition of fibres results in a change in the mechanical behaviour of earthen composites, which then exhibit ductile behaviour. Whereas raw earth shows complete failure at maximum stress (around 2% strain), the specimens with fibres present large deformation capacities after the peak is reached (up to 5% strain as shown in Figure 8). Fibres can resist and delay failure by keeping the specimen in one piece thanks to adhesion properties between fibres and earth. Even though the addition of fibres causes a decrease in tensile strength due to the weak bonds between the fibres and the earthen matrix, fibres form bridges across cracks, which may have appeared during the failure phase. However, in order to have fibres resisting tension and well anchored into earth, the necessary anchor length, is provided by long fibres, and particularly by reed fibres in the present mix. Fibre content and length appear to affect flexural behaviour: when fibres have good tensile strength, good adhesion with the soil matrix and are long enough to remain anchored, they tend to delay cracking and hold the specimen together after cracking starts.

In Figure 9, maximum tensile stress and ensuing strain values are significantly scattered, ranging from 1 to 3% for specimens without fibres and from 2 to 6% for specimens with fibres. Fibres, on the one hand, have a significant impact on the shift in the strain value at which maximum peak occurs, but, on the other hand, significantly affect material behaviour on peak downslope. The results obtained by different authors for maximum strength are summarised with mean values and variation coefficients, when they are determined, in the appendix (Table A2).

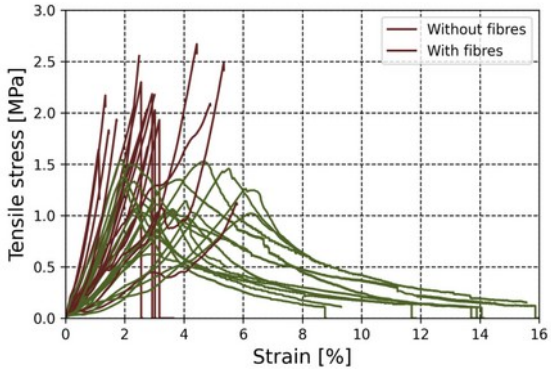

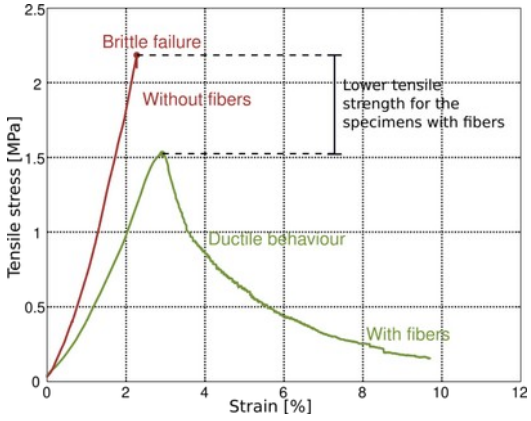

a) b)

Figure 9: Bending testing– experimental data obtained for 18 specimens (a) – focus on two representative curves to highlight differences between formulations with and without fibres (b)

4.1.2. Compression tests

Monotonic compression test results are presented in Figure 10-a for the 16 specimens tested. A focus has been placed on characteristic curve shape for both formulations in Figure 6 for specimens E2.1.4a (without fibres) and E1.2.1b (with fibres). During testing, compressive stress increases monotonically for the specimens with fibres and without fibres. The curves are fairly similar and non-linear in shape, which suggests that the behaviour of materials with or without fibres is not accurately elastic within the strain range tested here. This may be due to plastic deformation, damaged material and microstructural change caused by compression. Some specimens without fibres present non-monotonic stress variations for large strains, which may be explained by the presence of defects in the specimen, which then breaks, causing a sharp drop in stress and an increase in the strain up to 1.5%. After such events, compressive stress begins to rise again with the same slope than before, gained strain, however, is kept.

Figure 7-a presents the representative stress-strain curve obtained during cyclic compression testing for the specimen with fibres E1.2.4a. The curve shows the different stress levels applied during the different cycles. The envelope curve corresponds to the assumed monotonic compression test results. Before each cycle, a monotonic compression phase is applied, during which stress changes linearly with strain. Stress is then lowered to zero. During the unloading phase, strain also decreases but not according to the previous monotonic loading phase. During the last stage of the unloading phase, stress approaches 0. The slope value of the unloading phase is always higher than that of the loading phase. Stress is then increased to the prescribed value, increasing strain.

The 36 maximal compressive strength values (2 values for each specimen) obtained with both protocols (monotonic and cyclic) are displayed in Figures 10.b and 10.c.

Data analysis (Table 2) does not reveal any significant difference between the results obtained for specimens from the different slabs. The average value differences between both protocols are very small: 15% for raw earth specimens (3.2 MPa monotonic versus 2.7 MPa cyclic) and 10% for specimens with fibres (2.3 MPa monotonic versus 2.5 MPa cyclic). The lower compressive strength values obtained during cyclic compression testing may be accounted for by fatigue or damage, which may appear over successive loading/unloading loops and weakened material. The calculated CV is 20% for raw earth specimens (for both cyclic and monotonic protocols), whereas, regarding fibred specimens, it is 11% for the monotonic protocol and 33% for the cyclic one. Considering the small differences in CV between both protocols, it can therefore be concluded that compressive strength is not significantly affected by loading type (monotonic or cyclic). Given the consistency of data, it is decided to include all the results in the statistical analysis.

Similarly to tensile strength (but to a lesser extent), compressive strength values for specimens with fibres are lower than for specimens without fibres (2.4 MPa with fibres versus 2.9 MPa without fibres). Adding fibres reduces specimen strength but, as shown in Section 4.1.1, increases ductility. The findings presented in [28] for a high 3% to 6% mass ratios of barley and lavender straw fibres, show a reduction in compressive strength for fibred mixes. The results obtained in [14] show that compressive strength increases for up to 1.5% fibre content and decreases for higher fibre contents.

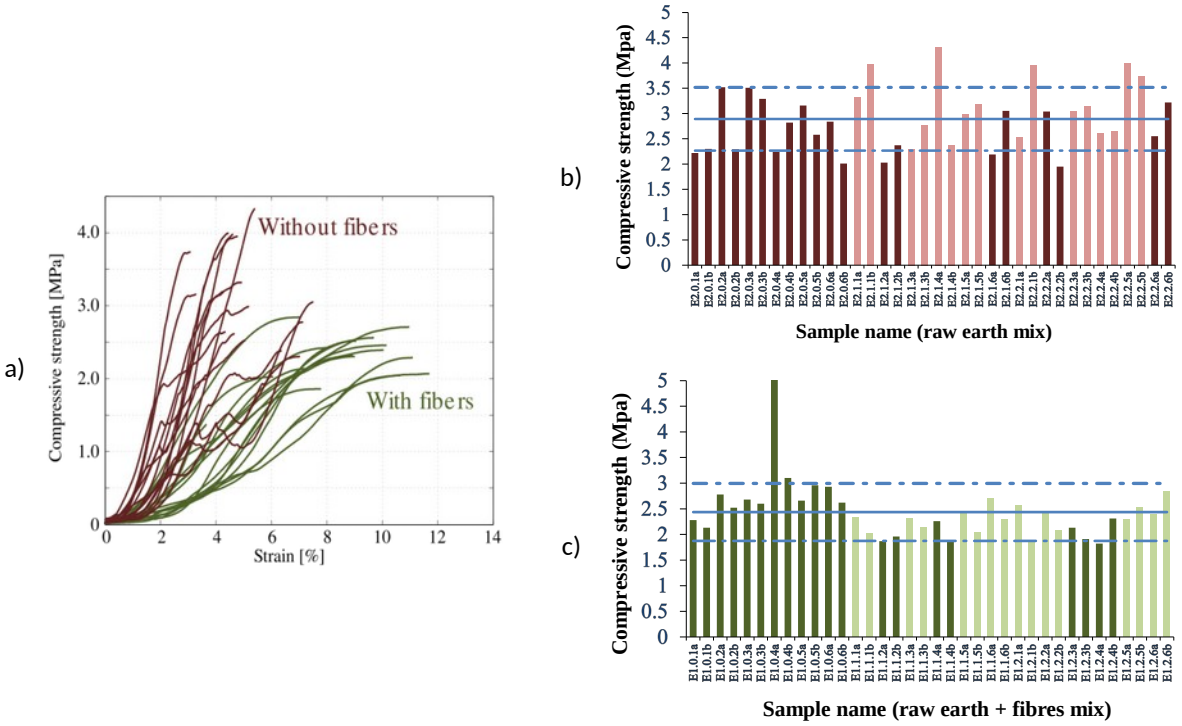

Figure 10: Monotonic loading curves (a) and compressive strength for raw earth specimens (b) and earth specimens with fibres (c) –specimen light-coloured results correspond to monotonic loading protocol

4.2. Statistical description

4.2.1. Compressive and tensile strengths

As shown in Figure 7, box plots have been used to illustrate the distribution of values over the variation range. In Figures 11 to 13, "S" values correspond to raw earth (soil only) specimens and "SF" values to composite (soil and fibres) specimens. Box plots obtained for tensile and compressive strengths are displayed in Figure 11-a and 11-b. The first three box plots correspond to data for specimens obtained from the three slabs (Slab 1, 2 and 3). The fourth box plot combines results for the three slabs (Slabs 1+2+3). Whatever the strength parameter considered (compressive or tensile), box plots reveal few outliers (1 for *Slab2 S* and *Slab3 SF* for tensile strength and 1 for *Slab3 SF* for compressive strength). For convenience, these outliers are not included in the calculation of the statistical indicators.

Regarding compressive strength, the variation range (excluding outliers) is larger for specimens without fibres than for specimens with fibres. Regarding tensile strength, on the other hand, the relative variation range is almost identical for both formulations. Yet, one could expect that fibre addition would increase material heterogeneousness and, thus, induce greater data dispersion around the average value, instead the opposite is observed. This observation can therefore be generalized as outliers are few for specimens with and without fibres.

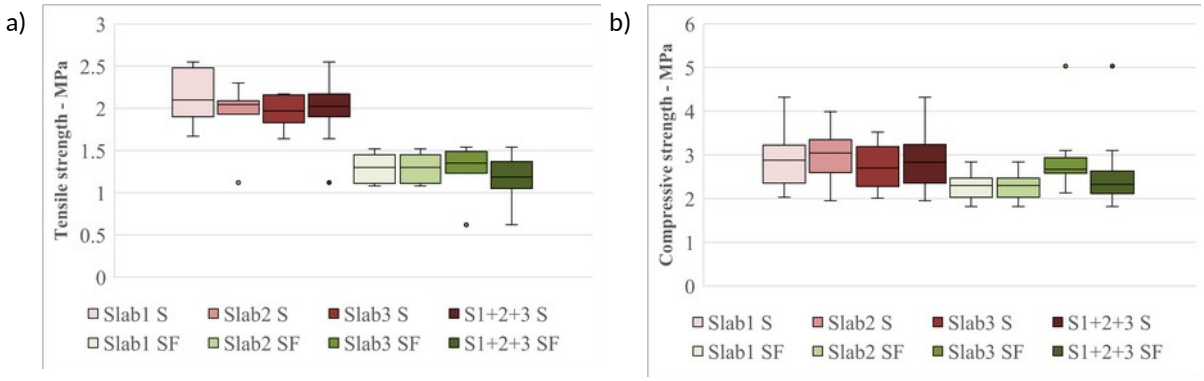

Figure 11: Box plots determined for tensile (a) and compressive (b) strengths for formulations with (green box plots) and without fibres (brown box plots) – dots correspond to outlier data

4.2.2. Young's modulus

This section presents the results obtained for:

- Young's modulus E_{mono} calculated from monotonic compression test data;
- Young's modulus E_{tan} calculated from cyclic compression test data on the ramp before the fifth stress level (approximately 60% of the specimen compressive strength);
- Young's modulus E_{cycle} calculated from cyclic compression test data for the different stress levels during loop unloading phase;
- Dynamic Young's modulus E_{dyn} measured with the Grindosonic apparatus, a non-destructive test device used for specimen measurements before bending testing begins.

Figure 12 presents the box plots corresponding to the Young's modulus determined during cyclic compression testing for both formulations and for the five different stress levels (cf. Section 8 for stress levels). Recall that each box plot processes 100 values (5 loops x 20 specimens). Material stiffness depends on loading characteristic history because Young's modulus evolves according to the stress level at which it is determined. Whatever the formulation, only two outlier values are measured at all the stress levels. Moreover, the scattering of values remains low. Because the Young's modulus of specimens with fibres is lower than that of specimens without fibres at all stress levels, the addition of fibres decreases material stiffness. Material stiffness could be expected to decrease during the loading phase where the material is damaged; on the contrary, it increases. This may be explained by a decrease in material porosity that counteracts defect initiation by increasing the number of contacts between soil aggregates and fibres and rearranging the grains.

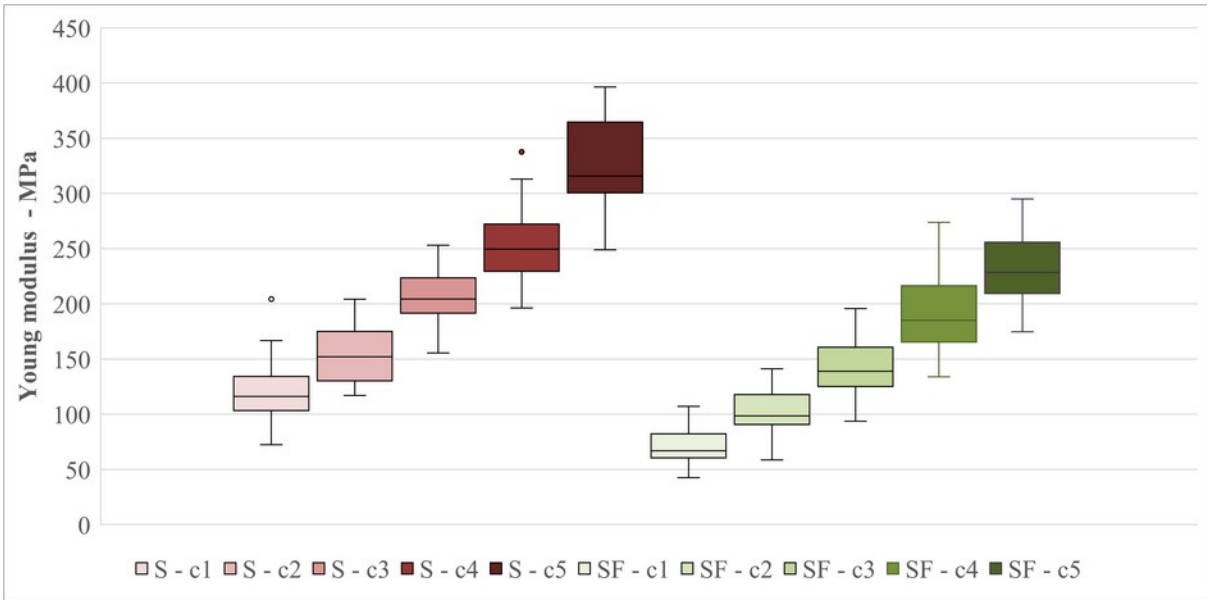

Figure 12: Evolution of statistical indicators for Young's modulus calculated during unloading phase for the different loops of cycles 1 to 5 (different stress levels) and for formulations with (green box plots) and without fibres (brown box plots)

Figure 13 presents box plots values for Young's modulus calculated from data obtained from:

- monotonic compression testing;
- the ramp before last cycle of cyclic compression testing;
- the different cycle loops for the highest stress level;
- Grindosonic testing (dynamic modulus).

Values for E_{tan} and E_{mono} are similar. However, scattering of values is larger for E_{tan}. As shown in Figure 7-b, the stress-strain curves recorded during cyclic compression testing are assumed to follow the envelope curves measured during monotonic compression testing and just adding cycle loops for prescribed stress levels. Outside the loops, curves are assumed to superimpose, although this cannot be proven because:

- Tests are destructive;
- Material characteristics change during testing and specimens cannot be reused after being subjected to heavy loading and high mechanical stress.

Nevertheless, Young's modulus close values obtained confirm that both methods provide similar information regarding material stiffness.

However, values obtained during the loop unloading phase of cyclic compression testing provide more reliable information. During monotonic compression or ramp testing, indeed, the material is subjected to compression strains, during which elastic and plastic deformations can combine. On the contrary, during the loop unloading phase within a given cycle, deformations are only elastic. Values of E_{cycle}, therefore, correspond to the material

elastic behaviour. They are greater and less scattered than E_{tan} and E_{mono} (lower interquartile range), which can probably be explained by the large amount of data. For the specimens with fibres, the median value of E_{cycle} is approximately twice that of E_{tan} and E_{mono}, while it is about three times greater for specimens without fibres. Material stiffness for cyclic compression testing is thus higher than for monotonic compression testing. This result reflects material compaction due to loading, which reduces porosity and increases stiffness. Consequently, loading at 60% of the ultimate strength would not damage specimens, but rather reinforce them.

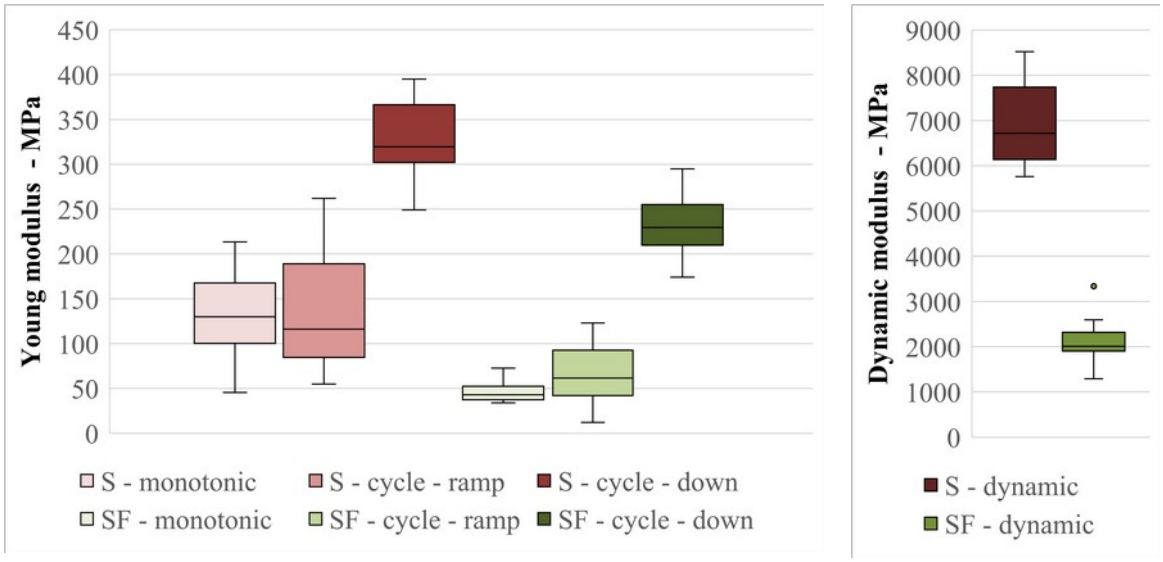

a) b)

Figure 13: Young's modulus: monotonic, cyclic – ramp, cyclic – unloading during 5th cycle (highest stress level), dynamic modulus

Figure 13 shows a comparison between Young's modulus obtained from cyclic compression test results and dynamic Young's modulus.

The values obtained from the mechanical tests are not of the same order of magnitude as those obtained from the non-destructive tests:

- Without fibres, the estimated average value is 6917MPa for dynamic Young's modulus and 327MPa for Young's modulus (approximately one twentieth of the dynamic value);
- With fibres, the estimated average value is 2088MPa for the dynamic Young's modulus and 232MPa for Young's modulus (approximately one ninth of the dynamic value).

The difference in value can be explained by differences in strain levels between press and Grindosonic testing. With the method using the Grindosonic device, strain levels are very low. As previously stated, soil behaviour is different at small or large strain levels [51].

In the literature, different correlations between dynamic and static moduli for concrete specimens and for rocks are discussed [52], [53]. Regarding soil, some correlations between Young's modulus and compressive strength are proposed in [54]. A survey of the literature reveals that no studies have been conducted to examine the correlation between dynamic and Young's moduli for earthen specimens used as building material. The relationship found in this analysis is linear and dependent on the presence of fibres (see figure 14). The slopes of the linear relationships between both moduli are not the same for the two formulations, which proves that differences cannot be represented by a single conversion coefficient related to the technique used, but may indicate some intrinsic behaviour differences of the material to wave propagation during Grindosonic testing.

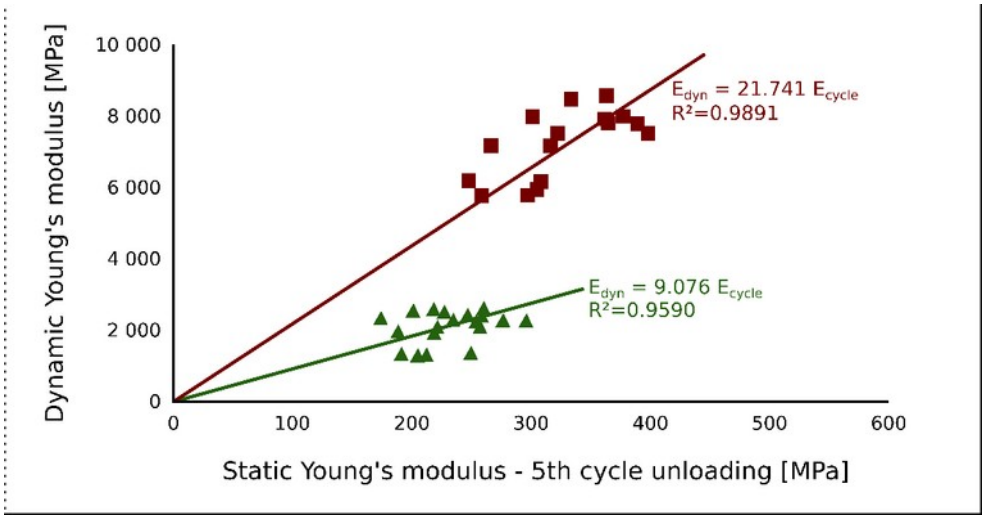

Figure *14*: Comparison between dynamic and static Young's moduli

4.3. Probability Density Functions (PDFs)

In this section, probability density functions for the different parameters studied are discussed. PDFs for each data set are determined according to procedures described in Section 12. A normal law fitted to each PDF is used to obtain values for mean μ and standard deviation σ. The resulting 5% percentile is also calculated. Depending on data scattering, the value obtained can be very different from the average value.

For all formulations and parameters tested, the tables presented in the following sections summarise:

- the mean value *m* calculated as experimental value simple mean;
- the coefficient of variation *CV* calculated as the ratio of experimental value standard deviation to mean value;
- the parameters of the fitted distribution law (μ and σ);
- the coefficient of variation calculated as the σ-to-μ ratio of the fitted distribution law*;*
- the 5th percentile value $f_{5\%}$ and the ratio of the fifth percentile to μ used to quantify the difference between $f_{5\%}$ and μ *(*when standard deviation is small, this value should be close to 100%, and close to 0% for highly scattered values).

4.3.1. Tensile strength

Figure 15 shows the PDFs determined for the tensile strength of specimens without fibres (a) and with fibres (b). Table 1 summarises the statistical indicators described above. Figure 16-b shows a comparison of the statistical indicators.

PDF for specimens without fibres, unlike those with fibres, is symmetrical and can be well described by a normal law. This may be explained by the fact that the number of specimens tested, although higher than most published articles, is not sufficient to obtain a Gaussian distribution. Indeed, according to the central limit theorem, the distribution of a large set of data for a given parameter, subject to multiple sources of random errors, as is the case for all the parameters here, must approximate a Gaussian distribution.

As mentioned previously, the mean value is higher for specimens with fibres and has a lower CV value. *m* and μ values are close for both formulations. CV calculated directly from experimental values and derived from PDF parameters is below 20%. The value for $f_{5\%}$ is 1.67MPa for specimens without fibres and 0.84MPa for specimens with fibres, i.e., 82% and 69% of the mean value, respectively. These values are slightly higher than the results obtained for adobe bricks reinforced with 0.64% cut straw [3], where $f_{5\%}/R_f$ reaches 50% ($f_{5\%}/R_f$=0.28MPa/0.56MPa = 50%).

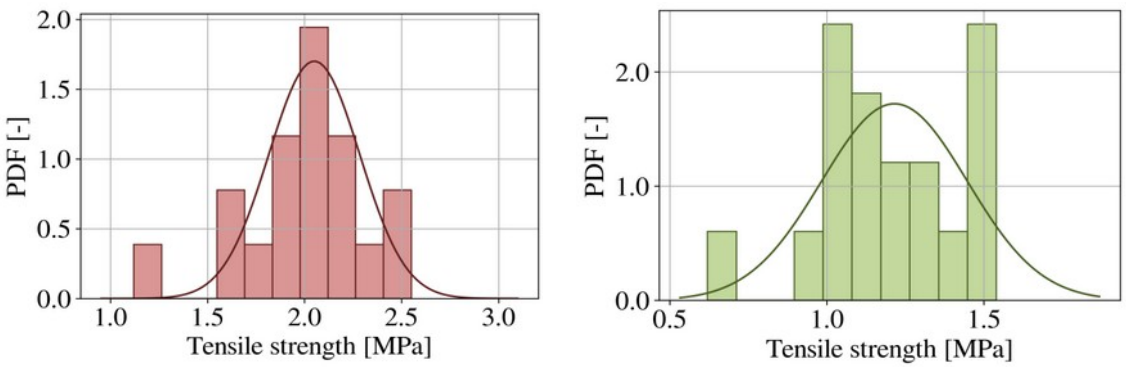

a) b)

Figure 15: PDF-s vs. tensile strength – specimens without fibres (a) and with fibres (b)

Table 1 – PDF parameters for tensile strength

Tensile strength							
Composite	**Results**		**Parameters of the fitted distribution law**			**5th percentile value**	**Ratio**
	Mean m	***CV***	***μ***	***σ***	*CV*	$f_{5\%}$	$f_{5\%}/\mu$
	MPa	%	MPa	MPa	%	MPa	**%**
Without fibres	2.00	16	2.05	0.23	11	1.67	82
With fibres	1.20	19	1.22	0.23	19	0.84	69

4.3.2. Compressive strength

Figures 17 to 19 display PDFs determined for compressive strength of specimens without fibres (a) and with fibres (b), and for the different test protocols (monotonic, cyclic) or for all the acquired data (monotonic+cyclic compression tests). Table 2 summarises the different statistical indicators calculated. Figure 16-a shows a comparison of the statistical indicators.

According to Sturges' law, the PDF pin number is higher than for tensile strength because the number of specimens tested is greater (twice the number). Regardless of the loading method used (monotonic or cyclic), compressive strength results summarised in Table 2 are lower when determined through PDF parameter optimization than when calculated from experimental data. Thus, using raw experimental data to derive mean and standard deviation could lead to an overestimate of both parameters. It is therefore advised to consider the relevance of PDF for the accurate estimate of both the mean and the standard deviation.

Moreover, the method (monotonic or cyclic) does not seem to have much influence on compressive strength values. However, it should be noted that the cyclic protocol is more relevant as it provides much more information about material mechanical behaviour and behaviour changes during testing. In addition, compressive strength determined for specimens without fibres presents an average value 20% higher when calculated using the monotonic instead of the cyclic protocol.

The published data discussed in Section 1 have CV values within the range 13%-51% for tensile strength, and 2%-95% for compressive strength. Variability is very high.

Calculated CV values presented in Table 2 are very close to those for hemp concrete compressive strength [40], and within the same range than those obtained for the thermal properties of earthen composites [20-21]. Yet, the results are higher than the values measured for mechanical and durability properties of cementitious materials (approximately 10%-18%) [48-49]. CV values can be used to assess measurement reliability [50]. Regarding concrete compressive strength variability, the authors in [50] propose accepted limits as a function of quality control between 10%-20%. The findings discussed here suggest that handmade earthen specimens are as homogeneous as on-site cast concrete specimens and that measured values can be considered reliable.

The results of $f_{5\%}/\mu$ are between 59%-80%. The lower values are obtained for specimens without fibres, which indicate that scattering is greater than for specimens with fibres, as noted above. This means that there is a large difference between the value engineers should use when assessing structural risk $f_{5\%}$, and mean value μ. Considering μ for this calculation instead of $f_{5\%,}$ would result in an overestimation of structural stability.

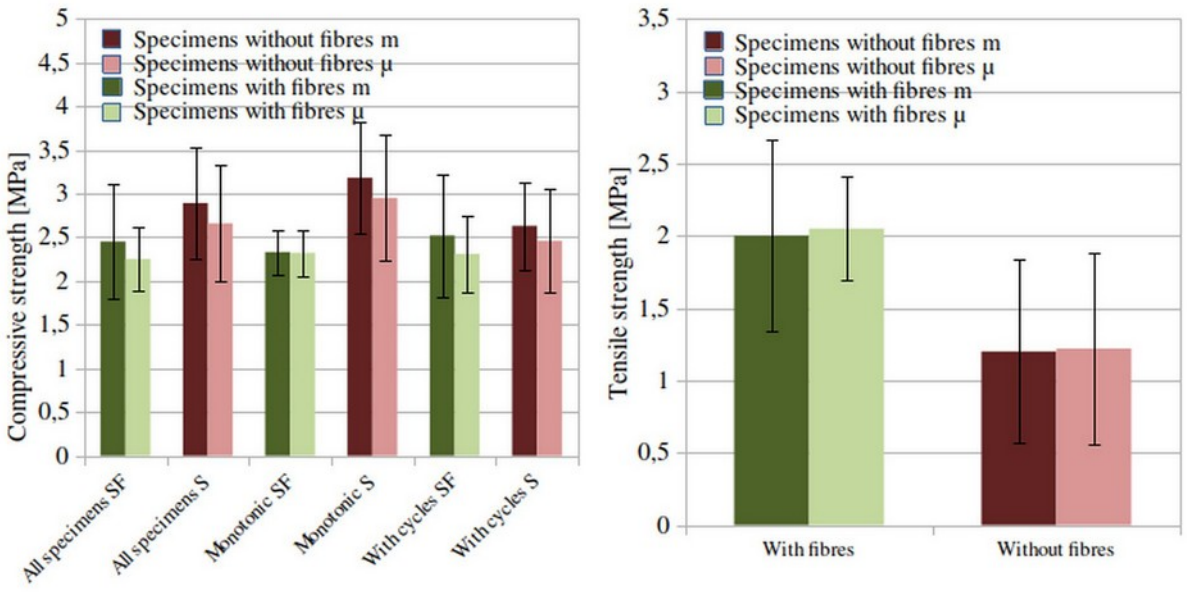

a) b)

Figure 16: Comparison between the mean value m and μ for compressive strength (a) and for tensile strength (b) – the error bars represent standard deviation

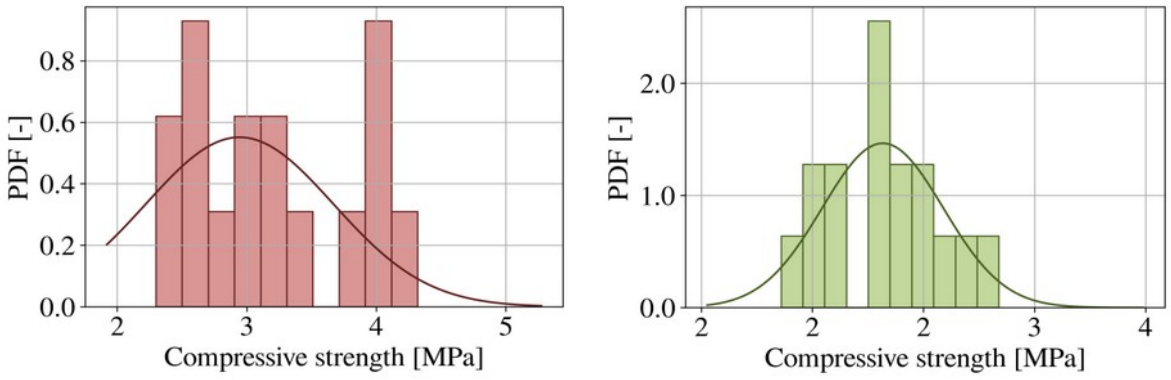

a) b)

Figure 17: PDF-s of compressive strength (monotonic testing protocol) – specimens without fibres (a) and with fibres (b)

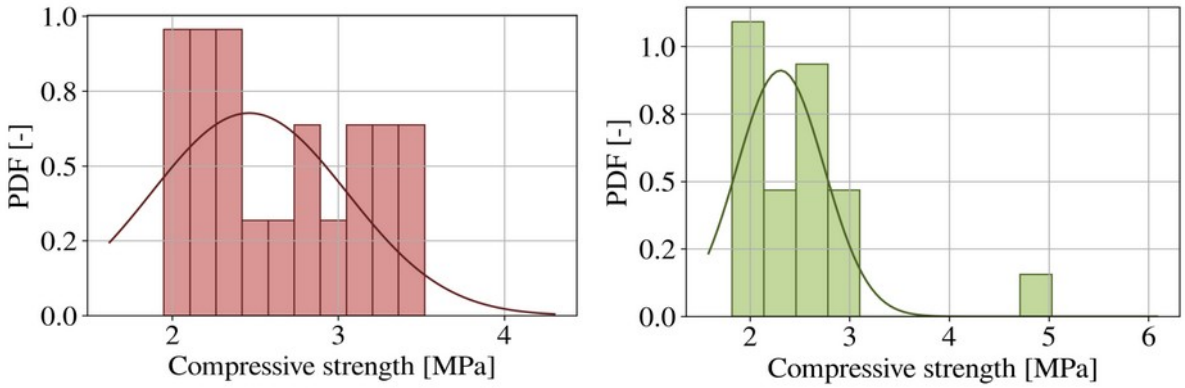

a) b)

Figure 18: PDF-s for compressive strength (testing protocol including cycles) – specimens without fibres (a) and with fibres (b)

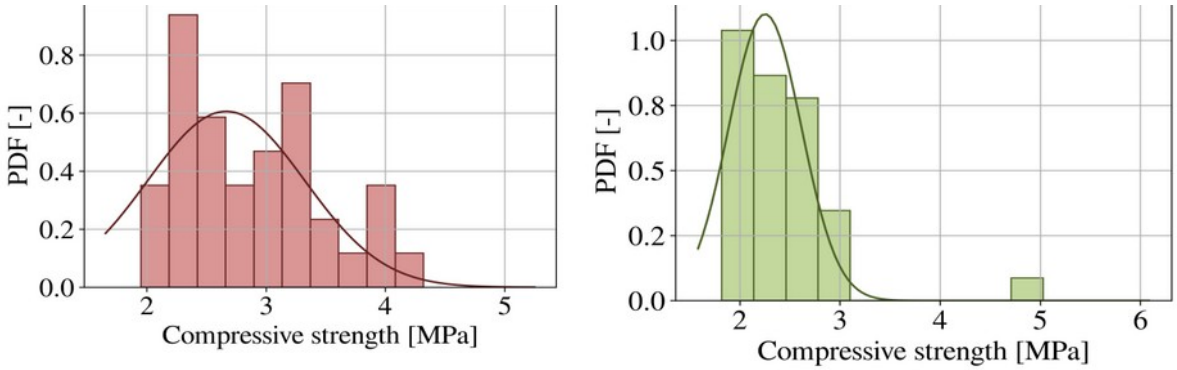

a) b)

Figure 19: PDF-s for compressive strength (all specimens) – specimens without fibres (a) and with fibres (b)

Table 2 – PDF parameters for compressive strength

Compressive strength								
Testing protocol	**Composite**	**Results**		**Parameters of the fitted distribution law**			**5th percentile value**	**Ratio**
		Mean m	***CV***	***μ***	***σ***	*CV*	$f_{5\%}$	$f_{5\%}/\mu$
		MPa	%	MPa	MPa	%	MPa	**%**
Monotonic	Without fibres	3.18	20	2.95	0.72	25	1.77	60
	With fibres	2.33	11	2.32	0.27	12	1.88	81
With cycles	Without fibres	2.63	19	2.46	0.59	24	1.49	61
	With fibres	2.52	28	2.31	0.44	19	1.59	69
All specimens	Without fibres	2.89	22	2.66	0.66	25	1.57	59
	With fibres	2.45	27	2.25	0.36	16	1.66	74

4.3.3. Young's modulus

Published Young's modulus data discussed in Section 1 are between 3%-139%. Yet, values found in the literature range from 21 to more than 10000 Mpa and differ widely. One must recall that, depending on the method used to determine Young's modulus, results within the same study (e.g., [23]) may show considerable disparities (by a factor of about 50).

Figure 20 displays PDFs for E_{mono}. Table 3 summarizes the parameters derived from the experimental data sets. Figure 23 presents a comparison of statistical indicators.

As previously mentioned, the average values of E_{tan} and E_{mono} are similar for both formulations. E_{cycle}, on the other hand, is higher by 144% for specimens without fibres and 303% for specimens with fibres. This substantial difference has already been discussed above.

It is essential to know which value structural designers should consider for calculations. E_{mono} or E_{tan} have similar values and can be easily obtained because monotonic compression testing is usually easy to perform. However, for reasons explained above, these results cannot fully be considered as Young's modulus values. However, it may be better to consider $f_{5\%}$ determined from E_{mono} or E_{tan}, because values are lower than for cyclic protocol (E_{cycle}) and would be regarded as an unfavourable case.

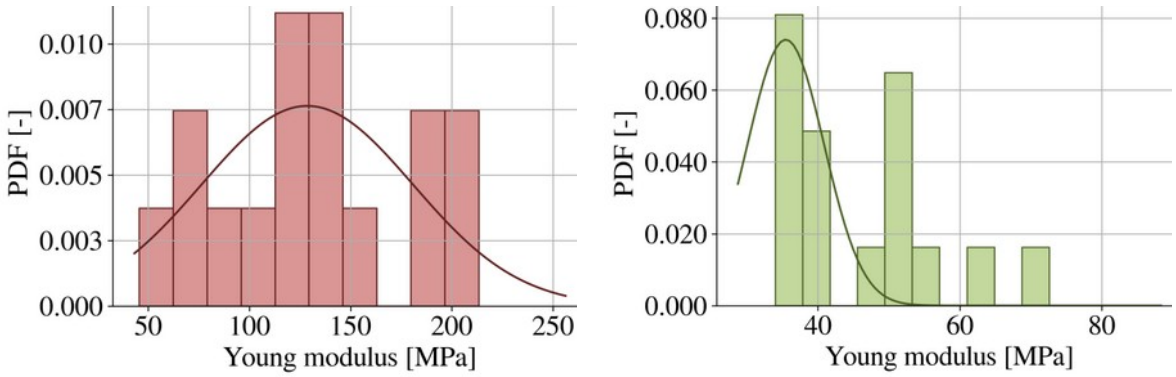

a) b)

Figure 20: PDF-s for Young's modulus based on monotonic protocol – specimens without fibres (a) and with fibres (b)

Table 3 – PDF parameters for Young's modulus based on monotonic protocol

Young's modulus based on monotonic protocol							
Composite	**Results**		**Parameters of the fitted distribution law**			**5th percentile value**	**Ratio**
	Mean m	***CV***	***μ***	***σ***	*CV*	$f_{5\%}$	$f_{5\%}/\mu$
	MPa	%	MPa	MPa	%	MPa	**%**
Without fibres	131	37	129	52	41	43	34
With fibres	46	24	35	5	15	27	77

Figure 21 displays PDFs for E_{tan} and Table 4 summarises corresponding parameters.

The distribution around the PDF mean value for Young's modulus is considerable. Coefficient of variation CV reaches values as high as 47% for specimens without fibres and 59% for specimens with fibres. Thus, experimental data and PDF corresponding values are similar for the formulation without fibres only.

The values of *m* and *μ* can also be very different. Considering *m* as the reference value, the relative difference between *m* and *μ* is 47% for specimens without fibres and 9% for specimens with fibres. The significant difference observed for raw earth specimens can be explained by the high peak appearing on the PDF curves around 50-75MPa (low values), on which the parameter optimization procedure centres PDFs. Calculation of *m* does not take into consideration the PDF shape.

Moreover, $f_{5\%}$ results can be very low compared to mean value *μ:* up to 17MPa for specimens without fibres and 2MPa for specimens with fibres, the standard deviation of the latter being particularly high. The large scatter observed may be due to the inaccuracy of the method or to the lack of relevance of E_{tan} for the description of material elastic behaviour, for the reasons explained above (elastic+plastic deformations).

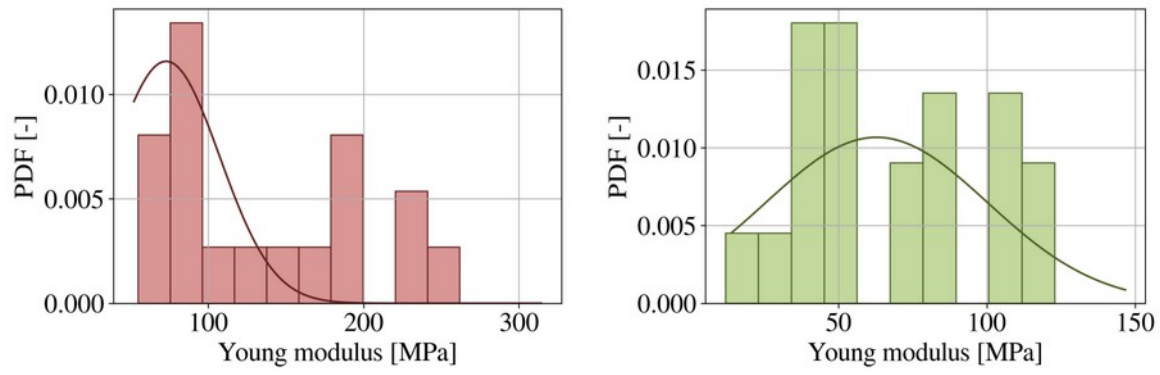

a) b)

Figure 21: PDF-s for Young's modulus E_{tan} based on cyclic protocol – calculated on ramp – specimens without fibres (a) and with fibres (b)

Table 4 – PDF parameters for Young's modulus based on cyclic protocol – calculated on ramp

Young's modulus based on cyclic protocol – calculated on ramp							
Composite	**Results**		**Parameters of the fitted distribution law**			**5th percentile value**	**Ratio**
	Mean m	***CV***	***μ***	***σ***	*CV*	$f_{5\%}$	$f_{5\%}/\mu$
	MPa	%	MPa	MPa	%	MPa	**%**
Without fibres	137	49	73	34	47	17	23
With fibres	69	48	63	37	59	2	3

Figure 22 displays PDFs for E_{cycle} and Table 5 summarises corresponding parameters. The number of values used to determine PDFs is high because they are calculated on the five loops of the last cycles (at 60% of total compressive strength) of the compression test carried out on 20 specimens for each formulation. Each PDF is thus determined from 100 values (the highest number of experimental values among the different parameters studied). This gives a good estimate of normal law parameters (μ and σ). The relative difference between m and μ is 1.8% for specimens without fibres and 5.7% for specimens with fibres. These results are the lowest among the different parameters studied. CV values are low (around 16-17% for both formulations). This low distribution gives a value of $f_{5\%}$ equal to 73-74% of the mean value μ for both formulations. The dispersion of E_{cycle} is therefore lower than for E_{tan} or E_{mono}. Furthermore, as already shown, the values of E_{cycle} are greater than E_{tan} or E_{mono}.

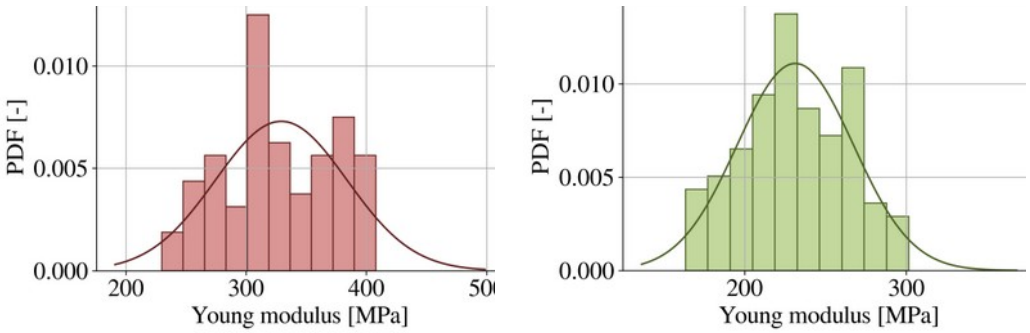

a) b)

Figure 22: PDF-s for Young's modulus based on cyclic protocol – calculated on cycle – specimens without fibres (a) and with fibres (b)

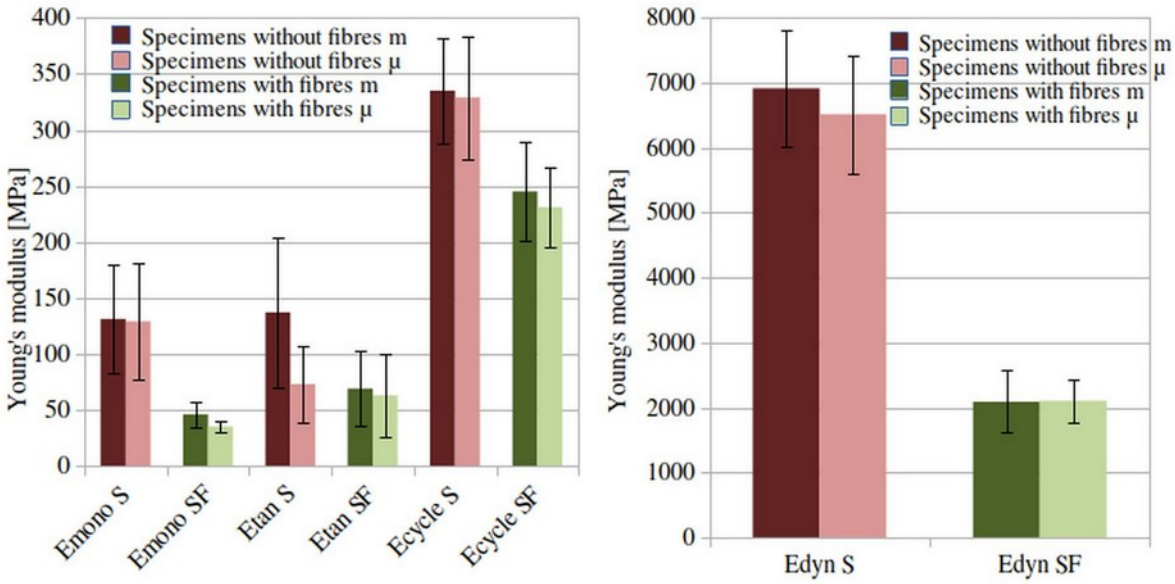

a) b)

Figure 23: Comparison of Young's modulus values determined according to the different test protocols static modulus (a) dynamic modulus (b) –error bars represent standard deviation

Table 5 – PDF parameters for Young's modulus based on cyclic protocol – calculated on cycle

Young's modulus based on cyclic protocol – calculated on cycle							
Composite	Results		Parameters of the fitted distribution law			5th percentile value	Ratio
	Mean m	***CV***	***μ***	***σ***	*CV*	$f_{5\%}$	$f_{5\%}/\mu$
	MPa	%	MPa	MPa	%	MPa	**%**
Without fibres	335	14	329	55	17	239	73
With fibres	245	18	231	36	16	172	74

Figure 24 displays PDFs for E_{dyn} and Table 6 summarises corresponding parameters. As mentioned above, dynamic Young's modulus values are much higher than those obtained with the different protocols (E_{tan}, E_{cycle}, E_{mono}). CV values are of the same order of magnitude as those observed for E_{cycle} (14% for formulation without fibres and 15% for formulation with fibres).

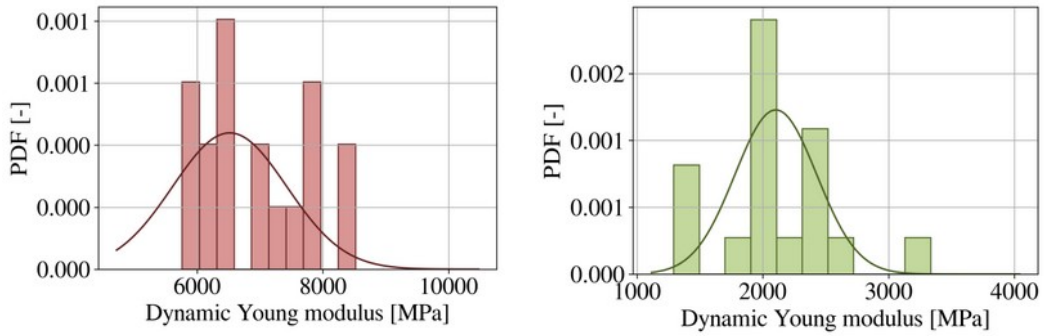

a) b)

Figure 24: PDF-s for dynamic modulus E_{dyn}

Table 6 – PDF parameters for dynamic modulus

Dynamic modulus E_{dyn}							
Composite	Results		Parameters of the fitted distribution law			5th percentile value	Ratio
	Mean m	***CV***	***μ***	***σ***	*CV*	$f_{5\%}$	$f_{5\%}/\mu$
	MPa	%	MPa	MPa	%	MPa	**%**
Without fibres	6917	13	6518	907	14	5026	77
With fibres	2088	23	2103	325	15	1568	75

5. Conclusions

Nowadays, the use of earthen composites seems an appropriate alternative to improve the environmental impact of the construction sector. Earth, indeed, is a locally-extracted and little processed material. However, even though this material is good choice for building construction, we need to improve our understanding of earth behaviour. In fact, there are no generally accepted regulations or standards available and there is no consensus on test methods for material property assessment, especially mechanical properties. On the basis of the results obtained, the following conclusions can be drawn:

- In the literature, the number of specimens tested is generally low and does not provide relevant statistical information on the different properties of earthen materials;
- Cyclic compression testing is recommended for the study of the earthen composite mechanical behaviour as this material exhibits non linear behaviour (elastic and plastic deformations, damage and porosity changes occur);
- Young's modulus E_{cycle} obtained during the unloading phase of the cyclic compression tests is more relevant than E_{tan} and E_{mono}, as it is determined during a phase when only elastic deformations occur;
- Young's modulus E_{cycle} increases as a function of applied stress, which confirms micro-structure changes within the material, likely due to a decrease in porosity;
- E_{dyn} is several orders of magnitude higher than E_{cycle}, probably because the strain levels induced using Grindosonic method are very low compared with those applied during compression testing;
- Testing carried out on a large number of specimen makes it possible to obtain average values and PDFs, from which various statistical indicators can be determined (standard deviation, COV, Q_1, Q_2 and Q_3 *quartiles*, *IQR*, outliers values, $f_{5\%}$,. . .);
- Results show that the value distribution can be considerable and that the difference between mean value and 5th percentile can be as high as 70%. This means that the risk of failure of earthen structures can be underestimated if building design is based on mean values.

Conflict of interest

None

Acknowledgements

This study has been conducted at the Institut de Recherche en Génie civil et Mécanique – CNRS UMR 6183, Saint Nazaire. The assistance and efforts of all those involved, in particular V. Schneider and N. Parois, Master Students from Nantes University, and D. Secarin and H. Khattabi, Master Students from Technical University of Civil Engineering of Bucharest, are sincerely appreciated. Part of the funds for the research work done by M. Barnaure was provided by a post-doctoral grant from the French Ministry for Foreign Affairs under reference 932566B/2018.

References

[1] Parisi, F., Asprone, D., Fenu, L., & Prota, A. (2015). Experimental characterization of Italian composite adobe bricks reinforced with straw fibres. Composite Structures, 122, 300-307.

[2] Fabbri A., Morel J.C., Aubert J.E., Quoc-Bao Bui, Gallipoli D., Ventura A., Venkatarama B.V. Reddy, Hamard E., Pelé-Peltier A., Holur Narayanaswamy Abhilash, An overview of the remaining challenges of the RILEM TC 274-TCE, testing and characterisation of earth-based building materials and elements, RILEM Technical Letters, 2022

[3] Loris Verron, Erwan Hamard, Bogdan Cazacliu, Andry Razakamanantsoa, Myriam Duc, Théo Vinceslas, Arthur Hellouin de Menibus, Blandine Lemercier, Rhoda Julia Ansaa-Asare, Thibaut Lecompte, Estimating and mapping the availability of earth resource for light earth building using a soil geo database in Brittany (France), Resources, Conservation and Recycling, Volume 184, 2022, 106409, ISSN 0921-3449, https://doi.org/10.1016/j.resconrec.2022.106409

[4] Rojat, F., Hamard, E., Fabbri, A., Carnus, B., & McGregor, F. (2020). Towards an easy decision tool to assess soil suitability for earth building. Construction and Building Materials, 257, 119544.

[5] Hamard, E., Lemercier, B., Cazacliu, B., Razakamanantsoa, A., & Morel, J. C. (2018). A new methodology to identify and quantify material resource at a large scale for earth construction–Application to cob in Brittany. Construction and Building Materials, 170, 485-497.

[6] Wolfskill, L. S., Dunlop, W. A., & Callaway, B. M. (1970). Handbook for building homes of earth: Department of Housing and Urban Development. Office of International Affairs, Washington, DC.

[7] Middleton, G.F. (1987) (revised by Schneider, L.M.) Fourth Edition. Bulletin 5. Earth Wall Construction. North Ryde, Australia: CSIRO Division of Building, Construction and Engineering, 1992.

[8] Walker, P. (2002). The Australian earth building handbook. In The Australian Earth Building Handbook. SAI Global Limited.

[9] Volhard, F., & Röhlen, U. (2009). Earthen construction rules: Terms–building materials–components (Lehmbau Regeln: Begriffe–Baustoffe–Bauteile).
[10] Delgado, M. C. J., & Guerrero, I. C. (2007). The selection of soils for unstabilised earth building: A normative review. Construction and building materials, 21(2), 237-251.
[11] Champiré, F., Fabbri, A., Morel, J. C., Wong, H., & McGregor, F. (2016). Impact of relative humidity on the mechanical behavior of compacted earth as a building material. Construction and Building Materials, 110, 70-78.
[12] Meimaroglou, N., & Mouzakis, C. (2019). Cation Exchange Capacity (CEC), texture, consistency and organic matter in soil assessment for earth construction: The case of earth mortars. Construction and Building Materials, 221, 27-39.
[13] Laborel-Preneron, A., Aubert, J. E., Magniont, C., Tribout, C. & Bertron, A. (2016). Plant aggregates and fibers in earth construction materials: A review. Construction and building materials, 111, pp. 719-734.
[14] Bouhicha, M., Aouissi, F., & Kenai, S. (2005). Performance of composite soil reinforced with barley straw. Cement and concrete composites, 27(5), 617-621.
[15] Piattoni, Q., Quagliarini, E., & Lenci, S. (2011). Experimental analysis and modelling of the mechanical behaviour of earthen bricks. Construction and Building Materials, 25(4), 2067-2075.
[16] Danso, H., Martinson, D. B., Ali, M., & Williams, J. (2015a). Effect of fibre aspect ratio on mechanical properties of soil building blocks. Construction and Building Materials, 83, 314-319.
[17] Danso, H., Martinson, D. B., Ali, M., & Williams, J. (2015b). Physical, mechanical and durability properties of soil building blocks reinforced with natural fibres. Construction and Building Materials, 101, 797-809.
[18] Jové-Sandoval, F., Barbero-Barrera, M. M., & Medina, N. F. (2018). Assessment of the mechanical performance of three varieties of pine needles as natural reinforcement of adobe. Construction and Building Materials, 187, 205-213.
[19] Cárdenas-Haro, X., Todisco, L., & León, J. (2021). Database with compression and bending tests on unbaked earth specimens and comparisons with international code provisions. Construction and Building Materials, 276, 122232.
[20] Barnaure, M., Bonnet, S., & Poullain, P. (2021). Earth buildings with local materials: Assessing the variability of properties measured using non-destructive methods. Construction and Building Materials, 281, 122613.
[21] Tchiotsop J., Issaadi N., Poullain P., Bonnet S., Belarbi R. (2022), Assessment of the natural variability of cob buildings hygric and thermal properties at material scale: Influence of plants add-ons, Construction and Building Materials, vol 342 b, doi.org/10.1016/j.conbuildmat.2022.127922
[22] Illampas, R., Ioannou, I., & Charmpis, D. C. (2014). Adobe bricks under compression: experimental investigation and derivation of stress–strain equation. Construction and Building Materials, 53, 83-90.
[23] Rodríguez-Mariscal, J. D., Solís, M., & Cifuentes, H. (2018). Methodological issues for the mechanical characterization of unfired earth bricks. Construction and Building Materials, 175, 804-814.
[24] Azil, A., Le Guern, M., Touati, K., Sebaibi, N., Boutouil, M., Streiff, F., Goodhew, S & Gomina, M. (2022). Earth construction: Field variabilities and laboratory reproducibility. Construction and Building Materials, 314, 125591.
[25] Miccoli, L., Müller, U. & Fontana, P. (2014). Mechanical behaviour of earthen materials: a comparison between earth block masonry, rammed earth and cob. Construction and Building Materials, 61, pp. 327-339.
[26] Silveira, D., Varum, H., Costa, A., Martins, T., Pereira, H. & Almeida, J. (2012). Mechanical properties of adobe bricks in ancient constructions. Construction and Building Materials, 28(1), pp. 36-44.
[27] Silveira, D., Varum, H., & Costa, A. (2013). Influence of the testing procedures in the mechanical characterization of adobe bricks. Construction and Building Materials, 40, 719-728.
[28] Giroudon, M., Laborel-Préneron, A., Aubert, J. E., & Magniont, C. (2019). Comparison of barley and lavender straws as bioaggregates in earth bricks. Construction and Building Materials, 202, 254-265.
[29] Salih, M. M., Osofero, A. I., & Imbabi, M. S. (2020). Constitutive models for fibre reinforced soil bricks. Construction and building materials, 240, 117806.
[30] Aymerich, F., Fenu, L., & Meloni, P. (2012). Effect of reinforcing wool fibres on fracture and energy absorption properties of an earthen material. Construction and Building Materials, 27(1), 66-72.
[31] Aymerich, F., Fenu, L., Francesconi, L., & Meloni, P. (2016). Fracture behaviour of a fibre reinforced earthen material under static and impact flexural loading. Construction and Building Materials, 109, 109-119.
[32] Rios, A. J., & O'Dwyer, D. (2020). Experimental validation for the application of the flat jack test in cob walls. Construction and Building Materials, 254, 119148.

[33] DIN 1048-5:1991 Testing concrete - testing of hardened concrete (specimens prepared in mould) German Institute for Standardisation (Deutsches Institut für Normung)
[34] NF EN ISO 17892-4 :2018 Geotechnical investigation and testing – Laboratory testing of soil – Part 4 : Determination of particle size distribution – Reconnaissance et essais géotechniques – Essais de laboratoire sur les sols – Partie 4 : Détermination de la distribution granulométrie des particules – ISO (the International Organization for Standardization), European Committee for Standardization (CEN)
[35] Baize, D. (2000). Guide des analyses en pédologie, Seconde éd. 2000, INRA, Paris
[36] NF EN ISO 17892-12 :2018 Geotechnical investigation and testing – Laboratory testing of soil – Part 12 : determination of liquid and plastic limits – Reconnaissance et essais géotechniques – Essais de laboratoire sur les sols – Partie 12 : Détermination des limites de liquidité et de plasticité – ISO (the International Organization for Standardization), European Committee for Standardization (CEN)
[37] NF EN 933-3+A1 :2013 Tests for geometrical properties of aggregates – Part 9 : assessment of fines – Methylene blue test - Essais pour déterminer les caractéristiques géométriques des granulats – Partie 9 : qualification des fines – Essai au bleu de méthylène European Committee for Standardization (CEN)
[38] Gourlay E, Glé P., Arnaud L. & Gourdon E. (2011). Multiphysical properties of hemp concretes, Matériaux & Techniques, 99, 625-631
[39] Gomes, M. I., Faria, P., & Gonçalves, T. D. (2019). Rammed earth walls repair by earth-based mortars: The adequacy to assess effectiveness. Construction and Building Materials, 205, 213-231.
[40] Niyigena, C., Amziane, S., Chateauneuf, A., Arnaud, L., Bessette, L., Collet, F., ... & Walker, P. (2016). Variability of the mechanical properties of hemp concrete. Materials Today Communications, 7, 122-133.
[41] Niyigena, C., Amziane, S., Chateauneuf, A. (2019). Assessing the impact of calculation methods on the variability of Young's modulus for hemp concrete material. Construction and Building Materials, 198, 332-344.
[42] Xu L, Kwai Kwan Wong, Fabbri A., Champiré F., Branque D. (2018). Loading-unloading shear behavior of rammed earth upon varying clay content and relative humidity conditions. Soils and Foundations, 58(4), pp 1001-1015. https://doi.org/10.1016/j.sandf.2018.05.005.
[43] Allison, R. J. (1987). Non-destructive determination of Young's modulus and its relationship with compressive strength, porosity and density. Geological Society, London, Special Publications, 29(1), 63-69.
[44] ASTM E1876-01, Standard Test Method for Dynamic Young's Modulus, Shear Modulus, and Poisson's Ratio by Impulse Excitation of Vibration, ASTM International, West Conshohocken, PA, 2001.
[45] Sturges, H. A. (1926). The choice of a class interval. Journal of the American Statistical Association, 21(153), 65-66.
[46] NF EN 1990: 2003 Eurocode 0: Basis of structural design, European Committee for Standardization (CEN)
[47] Laibi, A. B., Poullain, P., Leklou, N., Gomina, M., & Sohounhloué, D. K. (2018). Influence of the kenaf fibre length on the mechanical and thermal properties of Compressed Earth Blocks (CEB). KSCE Journal of Civil Engineering, 22(2), 785-793.
[48] Almeida Filho F.M., Barragán B.E., Casas J.R., El Debs A.L.H.C., (2010) Hardened properties of self-compacting concrete — A statistical approach, Construction and Building Materials 24 (2010) 1608–1615, doi:10.1016/j.conbuildmat.2010.02.032
[49] Bonnet S. & Balayssac J.P. (2018) Combination of the Wenner resistivimeter and Torrent permeameter methods for assessing carbonation depth and saturation level of concrete, Construction and Building Materials, 188, pp. 1149–1165.
[50] Melchers RE. (1987) Structural reliability: Analysis and prediction. Ellis Horwood Limited.
[51] Clayton, C. R. I. (2011). Stiffness at small strain: research and practice. Géotechnique, 61(1), 5-37.
[52] Djerbi Tegguer, A., Bonnet, S., Khelidj, A. & Baroghel-Bouny, V. (2013). Effect of uniaxial compressive loading on gas permeability and chloride diffusion coefficient of concrete and their relationship. Cement and Concrete Research, 52, 131-139.
[53] Asef, M. R., & Farrokhrouz, M. (2017). A semi-empirical relation between static and dynamic elastic modulus. Journal of Petroleum Science and Engineering, 157, 359-363.
[54] Caporale, A., Parisi, F., Asprone, D., Luciano, R., & Prota, A. (2015). Comparative micromechanical assessment of adobe and clay brick masonry assemblages based on experimental data sets. Composite Structures, 120, 208-220.

Appendix

Table A1 - Published compressive strength values							
Reference	**specimen number**	**Type of fibres**	**Fibre**	**Fibre length**	**Sample size**	**Compressive strength**	
						Mean value	**CV**
			%	mm	mm – mm - mm	MPa	%
[1]	34	straw	0.6	70	70-70-70	1.02	36
[16]	10	wheat straw	3	74	145-140-100	2.7	nd
	10	pinus halepensis	3	99	145-140-100	3.2	nd
	10	pinea	3	118	145-140-100	3.3	nd
	10	pinaster	3	127	145-140-100	2.4	Nd
[23]	10	straw	nd	300	115-420-420	1.59	2
	10	none	-	-	240-115-72	5.21	3
	10	none	-	-	110-500-500	3.28	12
[13]	2	none	-	-	310-460-130	5.2	nd
	2	wheat straw	2	50	310-460-130	7.4	nd
	2	wheat straw	3	50	310-460-130	5.5	nd
	2	wheat straw	4	50	310-460-130	7.5	nd
	2	wheat straw	2	50	310-460-130	4.6	nd
	2	wheat straw	3	50	310-460-130	6.6	nd
	2	wheat straw	4	50	310-460-130	7.9	nd
	2	wheat straw	1	50	310-460-130	7.5	nd
	2	wheat straw	2	50	310-460-130	5.6	nd
	2	wheat straw	3	50	310-460-130	8.3	nd
	8	none	-	-	150-230-130	2.9	17
	8	wheat straw	2	50	150-230-130	2.7	21
	8	wheat straw	3	50	150-230-130	2.5	11
	8	wheat straw	4	50	150-230-130	2.6	15
	8	wheat straw	2	50	150-230-130	2.6	11
	8	wheat straw	3	50	150-230-130	2.4	26
	8	wheat straw	4	50	150-230-130	2.8	9
	8	wheat straw	1	50	150-230-130	2.1	19
	8	wheat straw	2	50	150-230-130	2.4	16
	8	wheat straw	3	50	150-230-130	2.5	12
[21]	7	none	-	-	80-80-80	0.98	11
	7	none	-	-	80-80-80	1.13	17
	22	none	-	-	80-80-160	1.06	16
	5	none	-	-	Φ150-300	1.33	12
[24]	5	nd	nd	nd	Φ90-160	1.24	20*
	5	nd	nd	nd	Φ90-160	1	50*
	5	nd	nd	nd	Φ90-160	0.75	40*

	5	nd	nd	nd	Φ90-160	0.66	45*
	5	nd	nd	nd	Φ90-160	2.15	81*
	5	nd	nd	nd	Φ90-160	0.7	57*
	5	nd	nd	nd	Φ90-160	1.98	61*
	5	nd	nd	nd	Φ90-160	1.08	46*
	5	nd	nd	nd	Φ90-160	0.94	53*
	5	nd	nd	nd	Φ90-160	0.83	72*
	5	nd	nd	nd	Φ90-160	0.99	40*
	5	nd	nd	nd	Φ90-160	1.72	35*
	5	nd	nd	nd	Φ90-160	1.25	48*
	5	nd	nd	nd	Φ90-160	0.8	50*
	5	nd	nd	nd	Φ90-160	1.05	95*
	5	nd	nd	nd	Φ90-160	0.98	41*
[25]	7	nd	nd	nd	Φ90-160	0.78	24
	15	nd	nd	nd	Φ90-160	0.56	47
	6	nd	nd	nd	Φ90-160	0.41	28
	7	nd	nd	nd	110-110-110	0.9	31
	16	nd	nd	nd	100-100-100	0.42	29
	9	nd	nd	nd	100-100-100	0.47	16
[9]	4	none	-	-	Φ64-140	4	11*
	3	none	-	-	Φ64-140	2.9	9*
	4	none	-	-	Φ64-140	1.4	12*
	4	none	-	-	Φ64-140	4.7	13*
	3	none	-	-	Φ64-140	1	29*
	4	none	-	-	Φ64-140	2.2	30*
	4	none	-	-	Φ64-140	3.15	3*
	3	none	-	-	Φ64-140	1.9	12*
	4	none	-	-	Φ64-140	1.25	20*
[14]	5	coconut husk	1	40	290-140-100	1.35	3
	5	bagasse	1	80	290-140-100	1.1	3
	5	oil palm	1	38	290-140-100	1.14	2
[26]	3	none	-	-	Φ50-50	4.8	19
	3	barley straw	3	10	Φ50-50	3.3	6
	3	barley straw	6	10	Φ50-50	3.8	8
	3	lavender straw	3	8	Φ50-50	3.7	3
	3	lavender straw	6	8	Φ50-50	3.9	8
[20]	8	chopped straw	3	65	50-50-50	1.39	11
	8	chopped straw	3	65	50-50-50	0.66	77
	8	chopped straw	3	65	50-100-100	2.04	17
	5	chopped straw	3	65	50-100-100	0.45	4
	6	chopped straw	3	65	Φ50-50	0.85	3
	5	chopped straw	3	65	Φ50-50	1.02	17

	5	chopped straw	5	25	50-50-50	1.75	12
	5	chopped straw	5	25	50-50-50	1.47	22
	6	chopped straw	5	25	50-100-100	0.73	27
	8	chopped straw	5	25	50-100-100	1.88	13
	8	chopped straw	5	25	Φ50-50	1.34	28
	8	chopped straw	5	25	Φ50-50	1.41	21
[12]	4	none	-	-	220-107-60	4.1	nd
	4	barley straw	1	35	220-107-60	4.6	nd
	4	barley straw	1.5	35	220-107-60	4.9	nd
	4	barley straw	2	35	220-107-60	3.3	nd
	4	barley straw	2.5	35	220-107-60	2.9	nd
	4	barley straw	3	35	220-107-60	2.4	nd
	4	barley straw	3.5	35	220-107-60	2.2	nd
	4	none	-	-	220-107-60	5.1	nd
	4	barley straw	1	35	220-107-60	5.4	nd
	4	barley straw	1.5	35	220-107-60	5.6	nd
	4	barley straw	2	35	220-107-60	4.1	nd
	4	barley straw	2.5	35	220-107-60	3.7	nd
	4	barley straw	3	35	220-107-60	2.9	nd
	4	barley straw	3.5	35	220-107-60	2.7	nd
	4	none	-	-	220-107-60	4.5	nd
	4	barley straw	1	35	220-107-60	3.6	nd
	4	barley straw	1.5	35	220-107-60	3.1	nd
	4	barley straw	2	35	220-107-60	3	nd
	4	barley straw	2.5	35	220-107-60	2.3	nd
	4	barley straw	3	35	220-107-60	2.25	nd
	4	barley straw	3.5	35	220-107-60	2.2	nd
	4	none	-	-	220-107-60	4.2	nd
	4	barley straw	1	35	220-107-60	4.3	nd
	4	barley straw	1.5	35	220-107-60	4	nd
	4	barley straw	2	35	220-107-60	3.6	nd
	4	barley straw	2.5	35	220-107-60	3	nd
	4	barley straw	3	35	220-107-60	2.7	nd
	4	barley straw	3.5	35	220-107-60	2.6	nd
[27]**	5	chicken feather	0	15	50-50-50	3.88	nd
	5	chicken feather	1	15	50-50-50	3.45	nd
	5	chicken feather	3	15	50-50-50	2.98	nd
	5	chicken feather	5	15	50-50-50	3.05	nd
	5	chicken feather	7	15	50-50-50	4.14	nd
	5	chicken feather	9	15	50-50-50	2.91	nd
	5	chicken feather	11	15	50-50-50	2.02	nd

	5	bagasse	0	15	50-50-50	3.88	nd
	5	bagasse	1	15	50-50-50	3.21	nd
	5	bagasse	3	15	50-50-50	3.18	nd
	5	bagasse	5	15	50-50-50	3.9	nd
	5	bagasse	7	15	50-50-50	3.09	nd
	5	bagasse	9	15	50-50-50	2.92	nd
	5	bagasse	11	15	50-50-50	2.78	nd
*Computed by us from figures in the original paper ** Only values from tests at 180 days are shown in table. Tests were also performed at 14, 28, 56 and 90 days.							

Table A2 - Published tensile strength values resulting from bending testing							
Reference	**specimen number**	**Type of fibres**	**Fibre**	**Fibre length**	**Sample size**	**Tensile strength (3-point bending)**	
						Mean value	**CV**
			%	mm	mm - mm - mm	MPa	%
[1]	36	straw	0.6	70	40-160-40	0.56	36
[16]	5	wheat straw	3	74	290-140-100	0.14	nd
	5	pinus halepensis	3	99	290-140-100	0.22	nd
	5	pinea	3	118	290-140-100	0.17	nd
	5	pinaster	3	127	290-140-100	0.1	nd
[28]	4	wool	2	10	360-75-75	0.21	18*
	4	wool	2	20	360-75-75	0.23	16*
	4	wool	2	30	360-75-75	0.27	18*
	4	wool	3	10	360-75-75	0.24	13*
	4	wool	3	20	360-75-75	0.25	18*
	4	wool	3	30	360-75-75	0.28	25*
[29]	5	hemp	2	10	160x70x70	0.27	nd
	5	hemp	2	20	160x70x70	0.51	nd
	5	hemp	2	30	160x70x70	0.55	nd
	5	hemp	3	10	160x70x70	0.72	nd
	5	hemp	3	20	160x70x70	0.84	nd
	5	hemp	3	30	160x70x70	1.18	nd
[12]	4	none	-	-	280-70-70	2.5	nd
	4	barley straw	1.5	150	280-70-70	2.6	nd
	4	barley straw	2.5	150	280-70-70	2.7	nd
	4	barley straw	3.5	150	280-70-70	2.9	nd
	4	none	-	-	280-70-70	2	nd
	4	barley straw	1.5	150	280-70-70	1.9	nd
	4	barley straw	2.5	150	280-70-70	2.4	nd
	4	barley straw	3.5	150	280-70-70	2.5	nd
	4	none	-	-	280-70-70	1.1	nd
	4	barley straw	1.5	150	280-70-70	1.2	nd
	4	barley straw	2.5	150	280-70-70	1.7	nd
	4	barley straw	3.5	150	280-70-70	1.8	nd
	4	none	-	-	280-70-70	1.5	nd
	4	barley straw	1.5	150	280-70-70	1.5	nd
	4	barley straw	2.5	150	280-70-70	1.7	nd
	4	barley straw	3.5	150	280-70-70	2.1	nd
[25]	7	nd	nd	nd	410-240-120	0.72	35
	5	nd	nd	nd	460-240-110	0.48	51

	4	nd	nd	nd	430-220-120	0.41	24
[27]**	5	chicken feather	0	15	40-160-40	1.8	nd
	5	chicken feather	1	15	40-160-40	1.65	nd
	5	chicken feather	3	15	40-160-40	1.98	nd
	5	chicken feather	5	15	40-160-40	2.3	nd
	5	chicken feather	7	15	40-160-40	2.51	nd
	5	chicken feather	9	15	40-160-40	2.4	nd
	5	chicken feather	11	15	40-160-40	2.18	nd
	5	bagasse	0	15	40-160-40	1.8	nd
	5	bagasse	1	15	40-160-40	1.55	nd
	5	bagasse	3	15	40-160-40	1.75	nd
	5	bagasse	5	15	40-160-40	2.15	nd
	5	bagasse	7	15	40-160-40	1.89	nd
	5	bagasse	9	15	40-160-40	1.68	nd
	5	bagasse	11	15	40-160-40	1.62	nd

*Computed by us from figures in the original paper
** Only values from tests at 180 days are shown in table. Tests were also performed at 14, 28, 56 and 90 days.

Table A3 - Published modulus values based on different testing methodologies

Reference	Method for determining E	specimen number	Type of fibres	Fibre	Fibre length	Sample size	Modulus	
							Mean value	CV
				%	mm	mm x mm x mm	MPa	%
[1]	Secant modulus at one-third of peak strength $E_{1/3}$	34	straw	0.6	70	70-70-70	145	37
	Secant modulus at half of peak strength $E_{1/2}$	34	straw	0.6	70	70-70-70	143	40
[23]	DIN 1048-5 (Concrete testing; testing of hardened concrete - specimens prepared in mould)	10	straw	nd	300	420-420-115	651	68
		10	none	-	-	240-115-72	2197	3
		10	none	-	-	110-500-500	803	25
[13]	Not specified	2	none	-	-	310-460-130	94	nd
		2	wheat straw	2	50	310-460-130	71	nd
		2	wheat straw	3	50	310-460-130	71	nd
		2	wheat straw	4	50	310-460-130	59	nd
		2	wheat straw	2	50	310-460-130	66	nd
		2	wheat straw	3	50	310-460-130	58	nd
		2	wheat straw	4	50	310-460-130	73	nd
		2	wheat straw	1	50	310-460-130	74	nd
		2	wheat straw	2	50	310-460-130	80	nd
		2	wheat straw	3	50	310-460-130	66	nd
		8	none	-	-	150-230-130	211	45
		8	wheat straw	2	50	150-230-130	112	19
		8	wheat straw	3	50	150-230-130	108	21
		8	wheat straw	4	50	150-230-130	98	30
		8	wheat straw	2	50	150-230-130	119	29
		8	wheat straw	3	50	150-230-130	132	23
		8	wheat straw	4	50	150-230-130	108	43
		8	wheat straw	1	50	150-230-130	155	23
		8	wheat straw	2	50	150-230-130	139	25
		8	wheat straw	3	50	150-230-130	139	17
[21]	Between 1/3 and 2/3 of the compressive strength (E_m), displacement measured on the machine	7	none	-	-	80-80-80	60	16
		7	none	-	-	80-80-80	33	34
		22	none	-	-	80-80-160	132	35
		5	none	-	-	Φ150-300	195	11
	Between 0 and 1/3 of the compressive strength ($E_{1/3}$), displacement measured on the machine	7	none	-	-	80-80-80	47	72
		7	none	-	-	80-80-80	21	29
		22	none	-	-	80-80-160	77	34

		5	none	-	-	Φ150-300	78	28
	Between 0 and 2/3 of the compressive strength ($E_{2/3}$), displacement measured on the machine	7	none	-	-	80-80-80	47	23
		7	none	-	-	80-80-80	25	31
		22	none	-	-	80-80-160	95	32
		5	none	-	-	Φ150-300	111	27
	Between 1/3 and 2/3 of the compressive strength (E_m), displacement measured on the specimens	22	none	-	-	80-80-160	195	28
		5	none	-	-	Φ150-300	802	24
	Between 0 and 1/3 of the compressive strength ($E_{1/3}$), displacement measured on the specimens	22	none	-	-	80-80-160	1081	56
		5	none	-	-	Φ150-300	1539	52
	Between 0 and 2/3 of the compressive strength ($E_{2/3}$), displacement measured on the specimens	22	none	-	-	80-80-160	722	60
		5	none	-	-	Φ150-300	1005	24
[24]	Not specified	5	nd	nd	nd	Φ90-160	273	43*
		5	nd	nd	nd	Φ90-160	203	70*
		5	nd	nd	nd	Φ90-160	97	7*
		5	nd	nd	nd	Φ90-160	51	21*
		5	nd	nd	nd	Φ90-160	448	78*
		5	nd	nd	nd	Φ90-160	87	76*
		5	nd	nd	nd	Φ90-160	334	85*
		5	nd	nd	nd	Φ90-160	143	56*
		5	nd	nd	nd	Φ90-160	168	61*
		5	nd	nd	nd	Φ90-160	117	81*
		5	nd	nd	nd	Φ90-160	200	70*
		5	nd	nd	nd	Φ90-160	340	13*
		5	nd	nd	nd	Φ90-160	209	95*
		5	nd	nd	nd	Φ90-160	94	78*
		5	nd	nd	nd	Φ90-160	114	139*
		5	nd	nd	nd	Φ90-160	127	110*
[25]	Secant modulus at one-third of peak stress, deformations measured on specimens	4	nd	nd	nd	Φ90-160	9000	28
		3	nd	nd	nd	Φ90-160	15000	45
		3	nd	nd	nd	Φ90-160	17500	36
	Secant modulus at peak stress, deformations measured on specimens	4	nd	nd	nd	Φ90-160	1500	24
		3	nd	nd	nd	Φ90-160	2500	33
		3	nd	nd	nd	Φ90-160	2000	35
[26]	From the linear part of the stress-strain curves, not specified if displacements measured on the machine or on the specimen	3	none	-	-	Φ50-50	502	34
		3	barley straw	3	10	Φ50-50	62	5
		3	barley straw	6	10	Φ50-50	31	3
		3	lavender straw	3	8	Φ50-50	134	8
		3	lavender straw	6	8	Φ50-50	64	5
[20]	Secant modulus between 5% and 50% of maximum stress, deformations measured	94	chopped straw	3	65	50-50-50	32	72
		48	chopped straw	5	25	50-50-50	37	45

	on the machine							
[9]	Loading-reloading cycles at 20% of maximum expected stress level, displacements measured on specimen	3	none (rammed earth)	-	-	Φ64-140	2460	nd
	Loading-reloading cycles at 40% of maximum expected stress level, displacements measured on specimen	3	none (rammed earth)	-	-	Φ64-140	2230	nd
	Loading-reloading cycles at 60% of maximum expected stress level, displacements measured on specimen	3	none (rammed earth)	-	-	Φ64-140	2110	nd
	Loading-reloading cycles at 80% of maximum expected stress level, displacements measured on specimen	3	none (rammed earth)	-	-	Φ64-140	2000	nd
[30]	Double flat jack tests, slope of the elastic range of the material stress/ strain curves	5	wheat straw	1.5	400	400-1000-1000	176	49
	Double flat jack tests, secant modulus computed in accordance with ASTM C1197	5	wheat straw	1.5	400	400-1000-1000	203	43
[27]	Secant modulus at 1/3 or the peak strength	nd	chicken feather	nd	nd	50-50-50	1055	47
		nd	bagasse	nd	nd	50-50-50	881	38
*Computed by us from figures in the original paper								